

SUPPLEMENTARY DATA

for

Steroid-based gelator of A(LS)₂ type: Tuning gel formation by metal coordination

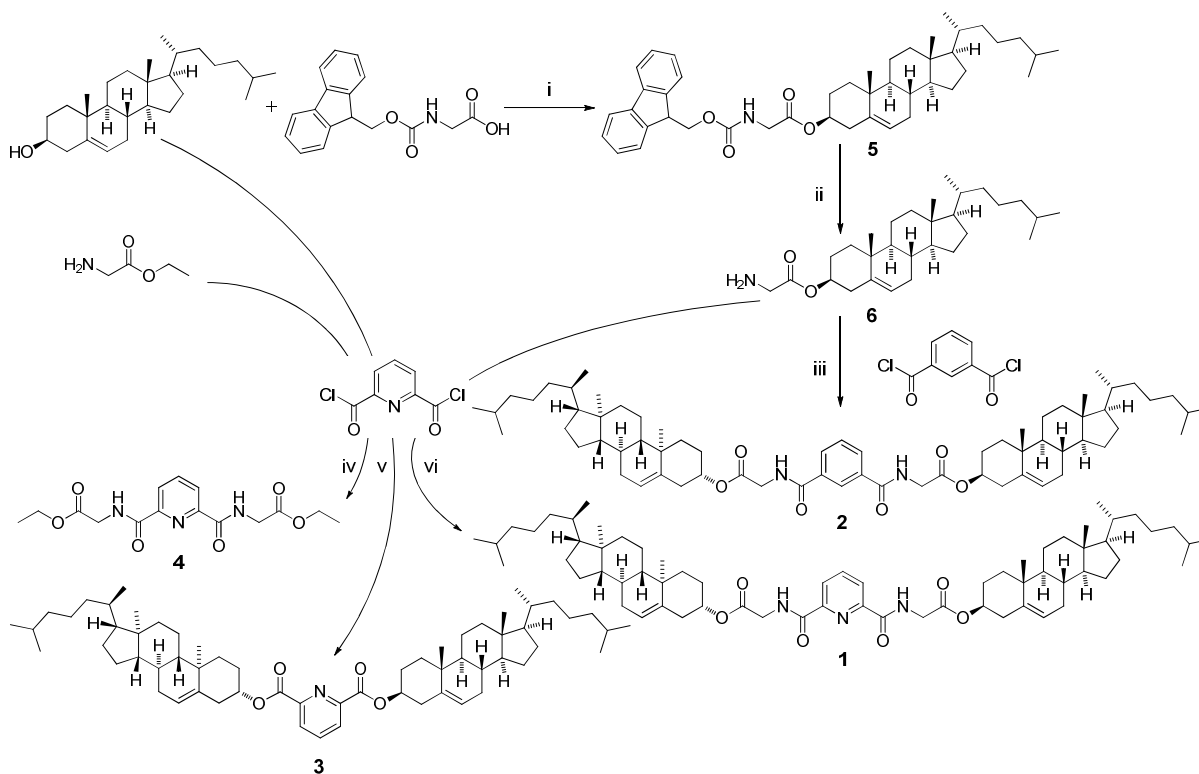
Hana Svobodová^{a,b}, Nonappa^a, Manu Lahtinen^a, Zdeněk Wimmer^{b,c} and Erkki Kolehmainen^a

^a *Department of Chemistry, University of Jyväskylä, P.O. Box 35, FIN-40014 University of Jyväskylä, Finland. Fax: +358 14 260 2501; E-mail: hana.svobodova@jyu.fi, erkki.t.kolehmainen@jyu.fi*

^b *Isotope Laboratory, Institute of Experimental Botany AS CR, v.v.i., Videnska 1083, 14220 Prague 4, Czech Republic*

^c *Department of Chemistry of Natural Compounds, Institute of Chemical Technology, Technicka 5, 16628 Prague 6, Czech Republic*

Synthesis



Scheme 1 Synthesis of compounds 1-6; (i) DCC, DMAP, CH_2Cl_2 , rt, 48 h; (ii) piperidine, DMF, rt, 1 h; (iii)-(vi) TEA, CH_2Cl_2 , rt, 16 h.

General

Analytical grade reagents and solvents were used for the synthesis, purification and gelation studies. Cholesterol, Fmoc-glycine, 2,6-pyridinedicarbonyl dichloride, and isophthaloyl dichloride were purchased from Sigma Aldrich. ^1H and ^{13}C NMR experiments were run with a Bruker Avance DRX 500 NMR spectrometer equipped with a 5 mm diameter broad band inverse probehead working at 500.13 MHz for ^1H and at 125.76 MHz for ^{13}C . NMR spectra were measured in CDCl_3 and the chemical shifts were referenced to the solvent signal ($\delta = 7.26$ ppm for ^1H , and $\delta = 77.0$ ppm for ^{13}C from internal TMS). The numbering of the steroidal part is according to the IUPAC rules. Molecular masses were measured either by using a Micromass LCT ESI-TOF mass spectrometer or by a VG AutoSpace 3500 HR-MS high resolution mass spectrometer. IR spectra were recorded on a Bruker Tensor 27 FTIR spectrometer.

Preparation of compound 5

Cholesterol (1.912 g, 4.847 mmol), Fmoc-glycine (1.470 g, 4.847 mmol), DCC (1.200 g, 5.816 mmol, 1.2 equiv.) and DMAP (0.180 g, 1.473 mmol, 0.3 equiv.) were dissolved in dry CH₂Cl₂ (40 mL). The mixture was stirred for 2 days at room temperature. Then the mixture was filtered and the filtrate was evaporated to dryness and purified by column chromatography on silica (CH₂Cl₂). The cholesteryl-Fmoc-glycinate was obtained as a white solid (2.710 g, 84 %). δ_{H} (500.13 MHz; CDCl₃): 0.69 (3H, s, 18-CH₃), 0.88 (6H, dd, $J = 2.1$; 6.6 Hz, 26-CH₃ + 27-CH₃), 0.93 (3H, d, $J = 6.5$ Hz, 21-CH₃), 1.02 (3H, s, 19-CH₃), 3.98 (2H, d, $J = 5.0$ Hz, Gly-CH₂), 4.25 (1H, dd, $J = 6.9$; 7.3 Hz, Fmoc-CH), 4.41 (2H, d, $J = 7.3$ Hz, Fmoc-CH₂), 4.71 (1H, m, 3-CH), 5.39 (1H, m, 6-CH), 7.31 (2H, dd, $J = 7.4$; 7.6 Hz, Fmoc-CH), 7.40 (2H, dd, $J = 7.4$; 7.6 Hz, Fmoc-CH), 7.61 (2H, d, $J = 7.4$ Hz, Fmoc-CH), 7.77 (2H, d, $J = 7.6$ Hz, Fmoc-CH). δ_{C} (125.7 MHz; CDCl₃): 11.84 (C-18), 18.71 (C-21), 19.25 (C-19), 21.02 (C-11), 22.54 (C-27), 22.78 (C-26), 23.83 (C-23), 24.26 (C-15), 27.70 (C-2), 27.99 (C-25), 28.19 (C-16), 31.84 (C-7), 31.88 (C-8), 35.76 (C-20), 36.19 (C-22), 36.55 (C-10), 36.89 (C-1), 38.01 (C-4), 39.51 (C-24), 39.72 (C-12), 42.31 (C-13), 43.00 (Gly), 47.14 (Fmoc), 50.02 (C-9), 56.16 (C-17), 56.68 (C-14), 67.18 (Fmoc), 75.41 (C-3), 119.95 (Fmoc), 122.97 (C-6), 125.07 (Fmoc), 127.04 (Fmoc), 127.68 (Fmoc), 139.28 (C-5), 141.29 (Fmoc), 143.84 (Fmoc), 156.23 (Fmoc), 169.38 (C=O, Gly); $\nu_{\text{max}}/\text{cm}^{-1}$: 3347w (NH), 2935s, 2867m (CH), 1725s (C=O), 1518m (NH, bending) and 1197s (C-O); m/z (ES⁺) 688.44 ([M+H]⁺); m/z (HR-ESI) 688.4356, [C₅₃H₆₇NO₄+H]⁺ requires 668.4342.

Preparation of compound 6

Compound **5** (1.900 g, 2.853 mmol) was dissolved in DMF (36 mL). Then piperidine (9 mL) was added. The mixture was stirred for 1 hour at room temperature. Then the solvents were removed under reduced pressure and the crude product was purified by column chromatography on silica (CH₂Cl₂:CH₃OH = 80:1). Cholesteryl glycinatate (**6**) was obtained as a white solid (1.212 g, 96 %). δ_{H} (500.13 MHz; CDCl₃): 0.67 (3H, s, 18-CH₃), 0.85 (6H, dd, $J = 2.2$; 6.6 Hz, 26-CH₃ + 27-CH₃), 0.90 (3H, d, $J = 6.6$ Hz, 21-CH₃), 1.01 (3H, s, 19-CH₃), 3.38 (2H, s, Gly-CH₂), 4.65 (1H, m, 3-CH), 5.37 (1H, m, 6-CH); δ_{C} (125.7 MHz; CDCl₃): 11.83 (C-18), 18.70 (C-21), 19.26 (C-19), 21.02 (C-

11), 22.52 (C-27), 22.77 (C-26), 23.82 (C-23), 24.25 (C-15), 27.77 (C-2), 27.98 (C-25), 28.19 (C-16), 31.85 (C-7), 31.88 (C-8), 35.76 (C-20), 36.18 (C-22), 36.56 (C-10), 36.95 (C-1), 38.11 (C-4), 39.50 (C-24), 39.73 (C-12), 42.30 (C-13), 44.21 (Gly), 50.04 (C-9), 56.16 (C-17), 56.68 (C-14), 74.55 (C-3), 122.77 (C-6), 139.48 (C-5), 173.58 (C=O, Gly); $\nu_{\max}/\text{cm}^{-1}$: 3399w, 3342w (NH), 2933s, 2860s (CH), 1732s (C=O), 1621w (NH, bending) and 1207s (C-O); m/z (ES⁺) 444.37 ([M+H]⁺); m/z (HR-ESI) 444.3842, [C₃₈H₅₇NO₂+H]⁺ requires 444.3842.

Preparation of compound 1

Cholesteryl glycinate (**6**) (0.600 g, 1.352 mmol, 2.05 equiv.) was dissolved in dry CH₂Cl₂ (10 mL). Then triethylamine (200 μ L) was added and the mixture was cooled to 0 °C. Then a solution of 2,6-pyridinedicarbonyl dichloride (0.135 g, 0.662 mmol, 1 equiv.) in dry CH₂Cl₂ (5 mL) was added dropwise at 0 °C to the system. The reaction mixture was stirred at room temperature overnight. After the reaction time, the solvents were evaporated and the crude product was purified by column chromatography on silica (CHCl₃). The compound **1** was obtained as a white solid (0.587 g, 87 %). δ_{H} (500.13 MHz; CDCl₃): 0.68 (6H, s, 18-CH₃), 0.86 (12H, dd, $J = 2.1$; 6.7 Hz, 26-CH₃ + 27-CH₃), 0.91 (6H, d, $J = 6.6$ Hz, 21-CH₃), 1.02 (6H, s, 19-CH₃), 4.16 (dd, $J = 5.5$; 18.1 Hz) + 4.26 (dd, $J = 5.9$; 18.1 Hz, 4H, Gly-CH₂), 4.69 (2H, m, 3-CH), 5.38 (2H, m, 6-CH), 7.86 (1H, t, $J = 7.8$ Hz, arom.), 8.16 (2H, d, $J = 7.5$ Hz, arom.), 8.44 (2H, bt, $J = 5.8$ Hz, NH); δ_{C} (125.7 MHz; CDCl₃): 11.86 (C-18), 18.74 (C-21), 19.27 (C-19), 21.06 (C-11), 22.53 (C-27), 22.77 (C-26), 23.91 (C-23), 24.27 (C-15), 27.72 (C-2), 27.98 (C-25), 28.20 (C-16), 31.84 (C-7), 31.91 (C-8), 35.81 (C-20), 36.21 (C-22), 36.56 (C-10), 36.99 (C-1), 38.04 (C-4), 39.51 (C-24), 39.77 (C-12), 41.52 (Gly), 42.34 (C-13), 50.04 (C-9), 56.25 (C-17), 56.74 (C-14), 75.63 (C-3), 123.02 (C-6), 124.96 (arom.), 138.73 (arom.), 139.30 (C-5.), 148.03 (arom.), 163.42 (C=O), 169.70 (C=O, Gly); $\nu_{\max}/\text{cm}^{-1}$: 3404w (NH), 2934s, 2868s (CH), 1742s (C=O, -O), 1681s, 1664s (C=O, -NH), 1527s (NH) and 1206s (C-O); m/z (ES⁺) 1040.87 ([M+Na]⁺); m/z (HR-ESI) 1040.7426, [C₃₈H₅₇NO₂+Na]⁺ requires 1040.7432.

Preparation of compound 2

Cholesteryl glycinate (**6**) (0.600 g, 1.352 mmol, 2.05 equiv.) was dissolved in dry CH₂Cl₂ (10 mL). Then triethylamine (200 μL) was added and the mixture was cooled to 0 °C. Then a solution of isophthaloyl dichloride (0.134 g, 0.660 mmol, 1 equiv.) in dry CH₂Cl₂ (5 mL) was added dropwise at 0 °C to the system. The reaction mixture was stirred at room temperature overnight. After the reaction time, the solvents were evaporated and the crude product was purified by column chromatography on silica (CHCl₃). The compound **2** was obtained as a white solid (0.598 g, 89 %). δ_H (500.13 MHz; CDCl₃): 0.67 (6H, s, 18-CH₃), 0.86 (12H, dd, *J* = 2.1; 6.6 Hz, 26-CH₃ + 27-CH₃), 0.91 (6H, d, *J* = 6.5 Hz, 21-CH₃), 1.02 (6H, s, 19-CH₃), 4.16 (dd, *J* = 5.9; 18.6 Hz) + 4.20 (dd, *J* = 5.9; 18.6 Hz, 4H, Gly-CH₂), 4.69 (2H, m, 3-CH), 5.38 (2H, m, 6-CH), 7.35 (2H, t, *J* = 7.8 Hz, NH), 7.38 (1H, t, *J* = 5.3 Hz, arom.), 7.85 (2H, dd, *J* = 1.6, 7.8 Hz, arom.), 8.13 (1H, s, arom.); δ_C (125.7 MHz; CDCl₃): 11.85 (C-18), 18.72 (C-21), 19.27 (C-19), 21.05 (C-11), 22.53 (C-27), 22.77 (C-26), 23.89 (C-23), 24.26 (C-15), 27.71 (C-2), 27.98 (C-25), 28.21 (C-16), 31.84 (C-7), 31.90 (C-8), 35.80 (C-20), 36.20 (C-22), 36.57 (C-10), 36.95 (C-1), 38.02 (C-4), 39.50 (C-24), 39.76 (C-12), 42.07 (Gly), 42.33 (C-13), 50.05 (C-9), 56.23 (C-17), 56.72 (C-14), 75.59 (C-3), 122.99 (C-6), 125.14 (arom.), 128.89 (arom.), 130.55 (arom.), 133.82 (arom.), 139.30 (C-5), 166.79 (C=O), 169.77 (C=O, Gly); ν_{max}/cm⁻¹: 3336w (NH₂), 2933s, 2867s (CH), 1739s (C=O, -O), 1666s, 1651s (C=O, -NH), 1532s (NH) and 1197s (C-O); *m/z* (ES⁺) 1039.84 ([M+Na]⁺); *m/z* (HR-ESI) 1039.7468, [C₃₈H₅₇NO₂+Na]⁺ requires 1039.7479.

Preparation of compound 3

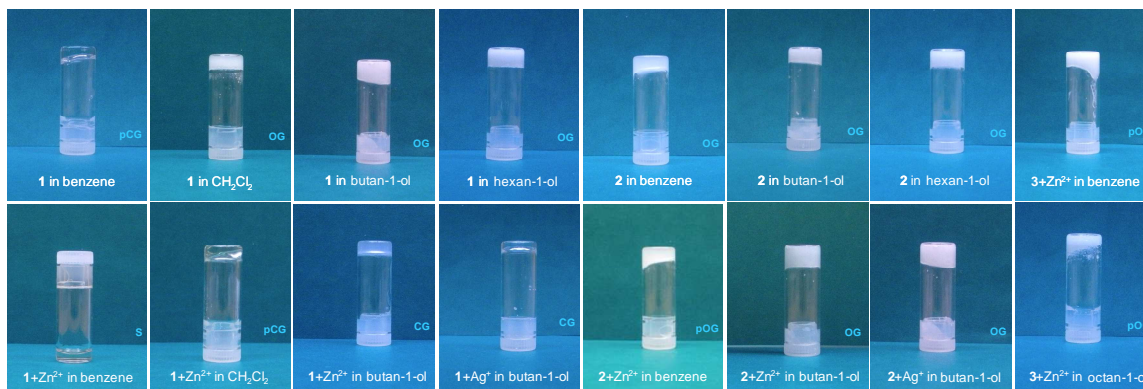
Cholesterol (1.000 g, 2.586 mmol, 2.05 equiv.) was dissolved in dry CH₂Cl₂ (10 mL). Then triethylamine (200 μL) was added and the mixture was cooled to 0 °C. Then a solution of 2,6-pyridinedicarbonyl dichloride (0.257 g, 1.260 mmol, 1 equiv.) in dry CH₂Cl₂ (10 mL) was added dropwise at 0 °C to the system. The reaction mixture was stirred at room temperature overnight. After the reaction time, the solvents were evaporated and the crude product was purified by column chromatography on silica (CHCl₃). The compound **3** was obtained as a white solid (1.008 g, 89 %). δ_H (500.13 MHz; CDCl₃): 0.69 (6H, s, 18-CH₃), 0.87 (12H, dd, *J* = 2.2; 6.6 Hz, 26-CH₃ + 27-

CH₃), 0.92 (6H, d, $J = 6.6$ Hz, 21-CH₃), 1.07 (6H, s, 19-CH₃), 4.92 (2H, m, 3-CH), 5.43 (2H, m, 6-CH), 7.96 (1H, t, $J = 7.8$ Hz, arom.), 8.23 (2H, d, $J = 7.6$ Hz, arom.); δ_C (125.7 MHz; CDCl₃): 11.86 (C-18), 18.72 (C-21), 19.35 (C-19), 21.06 (C-11), 22.54 (C-27), 22.79 (C-26), 23.84 (C-23), 24.29 (C-15), 27.66 (C-2), 28.00 (C-25), 28.22 (C-16), 31.90 (C-7), 31.94 (C-8), 35.79 (C-20), 36.20 (C-22), 36.67 (C-10), 37.05 (C-1), 38.00 (C-4), 39.53 (C-24), 39.77 (C-12), 42.34 (C-13), 50.09 (C-9), 56.18 (C-17), 56.72 (C-14), 76.19 (C-3), 122.95 (C-6), 127.57 (arom.), 137.92 (arom.), 139.55 (C-5.), 149.04 (arom.), 163.99 (C=O); $\nu_{\max}/\text{cm}^{-1}$: 2934s, 2866s (CH), 1739s (C=O, -O) and 1236s (C-O); m/z (ES⁺) 926.76 ([M+Na]⁺); m/z (HR-ESI) 926.6992, [C₃₈H₅₇NO₂+Na]⁺ requires 926.7003.

Preparation of compound 4

Glycine ethyl ester hydrochloride (0.300 g, 2.149 mmol, 2.07 equiv.) was dissolved in dry CH₂Cl₂ (10 mL). Then triethylamine (500 μ L) was added and the mixture was cooled to 0 °C. Then a solution of 2,6-pyridinedicarbonyl dichloride (0.212 g, 1.039 mmol, 1 equiv.) in dry CH₂Cl₂ (5 mL) was added dropwise at 0 °C to the system. The reaction mixture was stirred at room temperature overnight. After the reaction time, the solvents were evaporated and the crude product was purified by column chromatography on silica (CHCl₃). The compound **4** was obtained as an amorphous colorless solid (0.302 g, 86 %). δ_H (500.13 MHz; CDCl₃): 1.31 (6H, t, $J = 7.2$ Hz, ethyl-CH₃), 4.24 (2H, d, $J = 5.7$ Hz, Gly-CH₂), 4.26 (4H, q, $J = 7.2$ Hz, ethyl-CH₂), 7.96 (1H, t, $J = 7.9$ Hz, arom.), 8.25 (2H, d, $J = 7.8$ Hz, arom.), 8.35 (2H, bt, $J = 5.4$ Hz, NH); δ_C (125.7 MHz; CDCl₃): 14.13 (ethyl-CH₃), 41.42 (Gly), 61.63 (ethyl-CH₂), 125.17 (arom.), 138.87 (arom.), 148.17 (arom.), 163.53 (arom.), 170.03 (C=O); $\nu_{\max}/\text{cm}^{-1}$: 3336w (NH), 2982w, 2937w (CH), 1745s (C=O, -O), 1666s (C=O, -NH), 1524s (NH) and 1199s, 1176s (C-O); m/z (ES⁺) 360.17 ([M+Na]⁺); m/z (HR-ESI) 360.1179, [C₃₈H₅₇NO₂+Na]⁺ requires 360.1172.

Photographs of gels



Note: G = gel (O = opaque, C = clear transparent), pG = partial gel, S = solution.

Coordination studies

¹H NMR spectra were recorded with a Bruker Avance DPX 250 spectrometer equipped with a 5mm 1H/BB inverse detection probehead working at 250.13 MHz for ¹H.

Preliminary coordination studies of 1 and 2

	ligand (μL) (0.008 M, in CDCl ₃)	metal (μL) (0.08 M, in MeOD)	MeOD (μL)
1 or 2	400	0	200
1 or 2 + Ag(I) 2:1	400	20	180
1 or 2 + Ag(I) 1:5	400	200	0
1 or 2 + Zn(II) 2:1	400	20	180
1 or 2 + Zn(II) 1:5	400	200	0

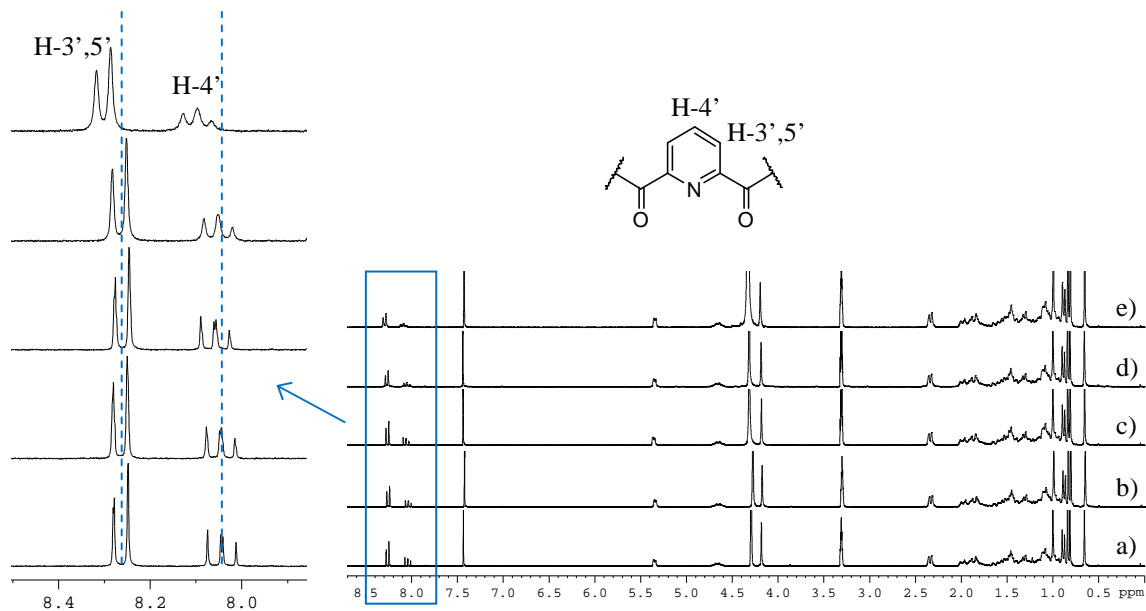


Fig. S1 ^1H NMR spectra of a) compound **1**, b) **1**+Ag(I) in ration 2:1, c) **1**+Ag(I) in ration 1:5, d) **1**+Zn(II) in ration 2:1, and e) **1**+Zn(II) in ration 1:5.

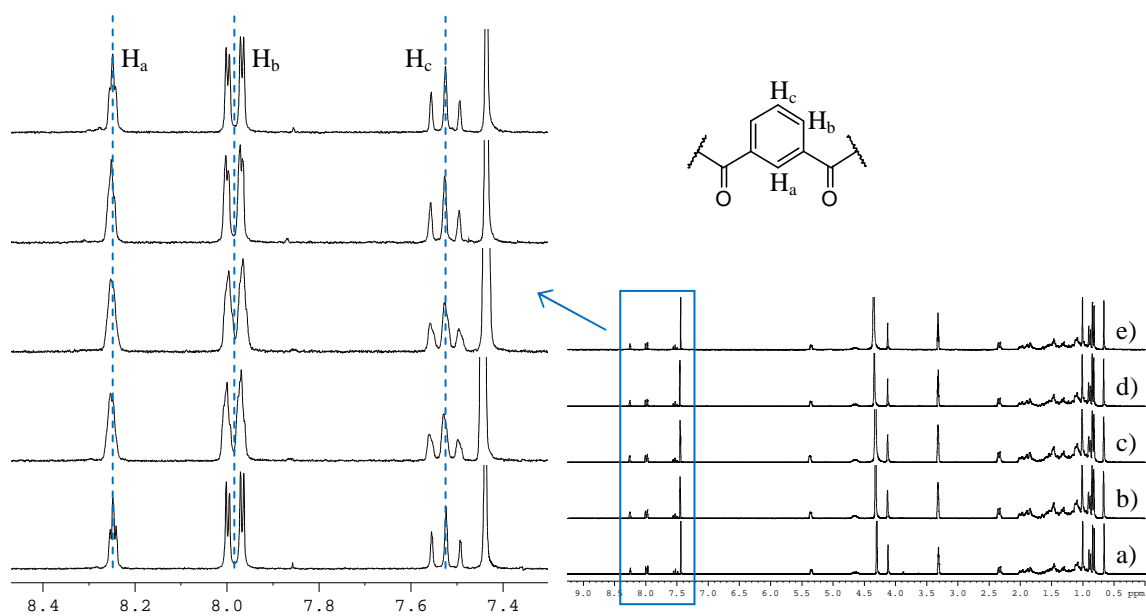


Fig. S2 ^1H NMR spectra of a) compound **2**, b) **2**+Ag(I) in ration 2:1, c) **2**+Ag(I) in ration 1:5, d) **2**+Zn(II) in ration 2:1, and e) **2**+Zn(II) in ration 1:5.

Job plot

Job's method of continuous variations was carried out for **1**+Ag(I) (Fig. S3) and **1**+Zn(II) (Fig. S4). ¹H NMR spectra in CDCl₃-CD₃OD (5:1) for **1**+Ag(I) and **1**+Zn(II), and in CDCl₃-CD₃CN (3:1) for **1**+Pd(II) were recorded for different ligand-metal ratios for the constant total concentration of 0.016 M (Fig. S5-S7).

Job plot of **1**+Ag(I)

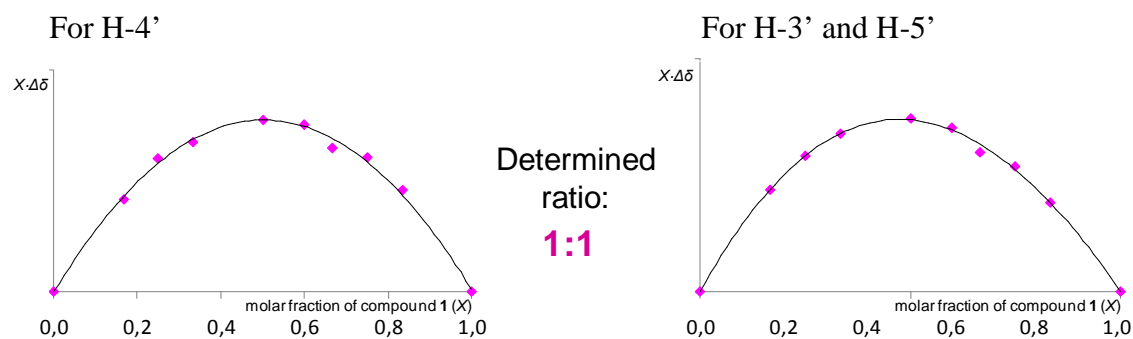


Fig. S3 Job plot analysis for **1**+Ag(I).

Job plot of **1**+Zn(II)

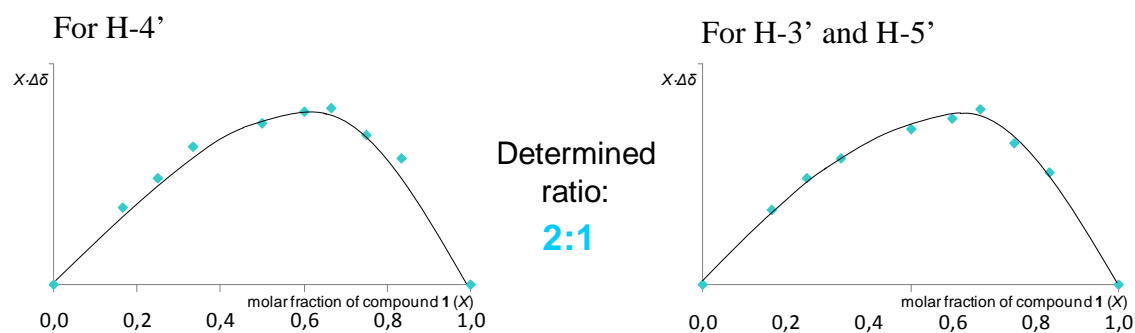


Fig. S4 Job plot analysis for **1**+Zn(II).

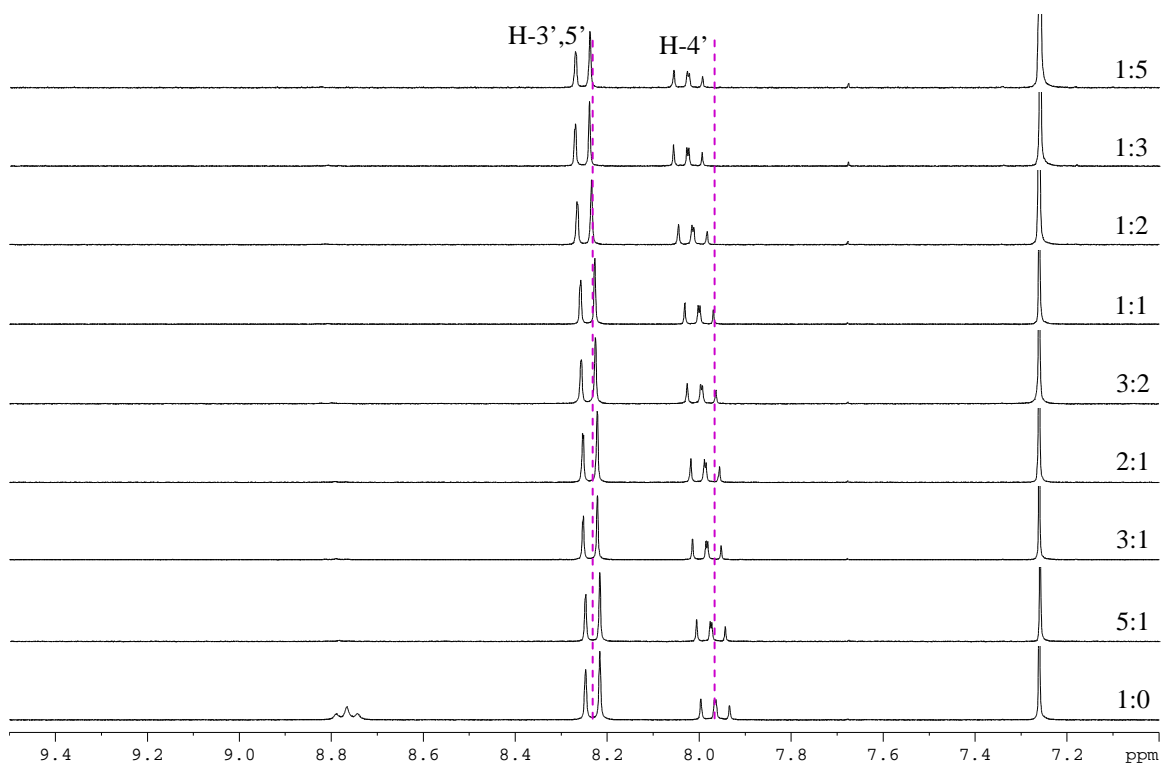
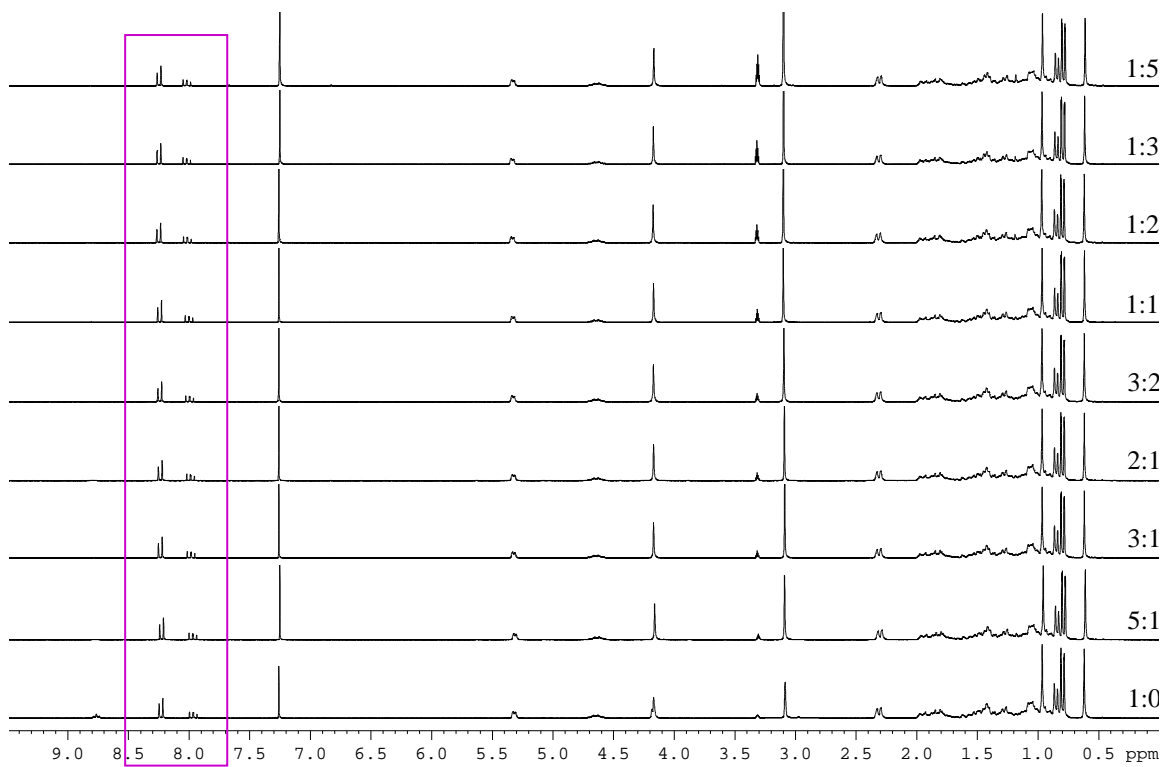


Fig. S5 ^1H NMR for Job plot of **1**+Ag(I).

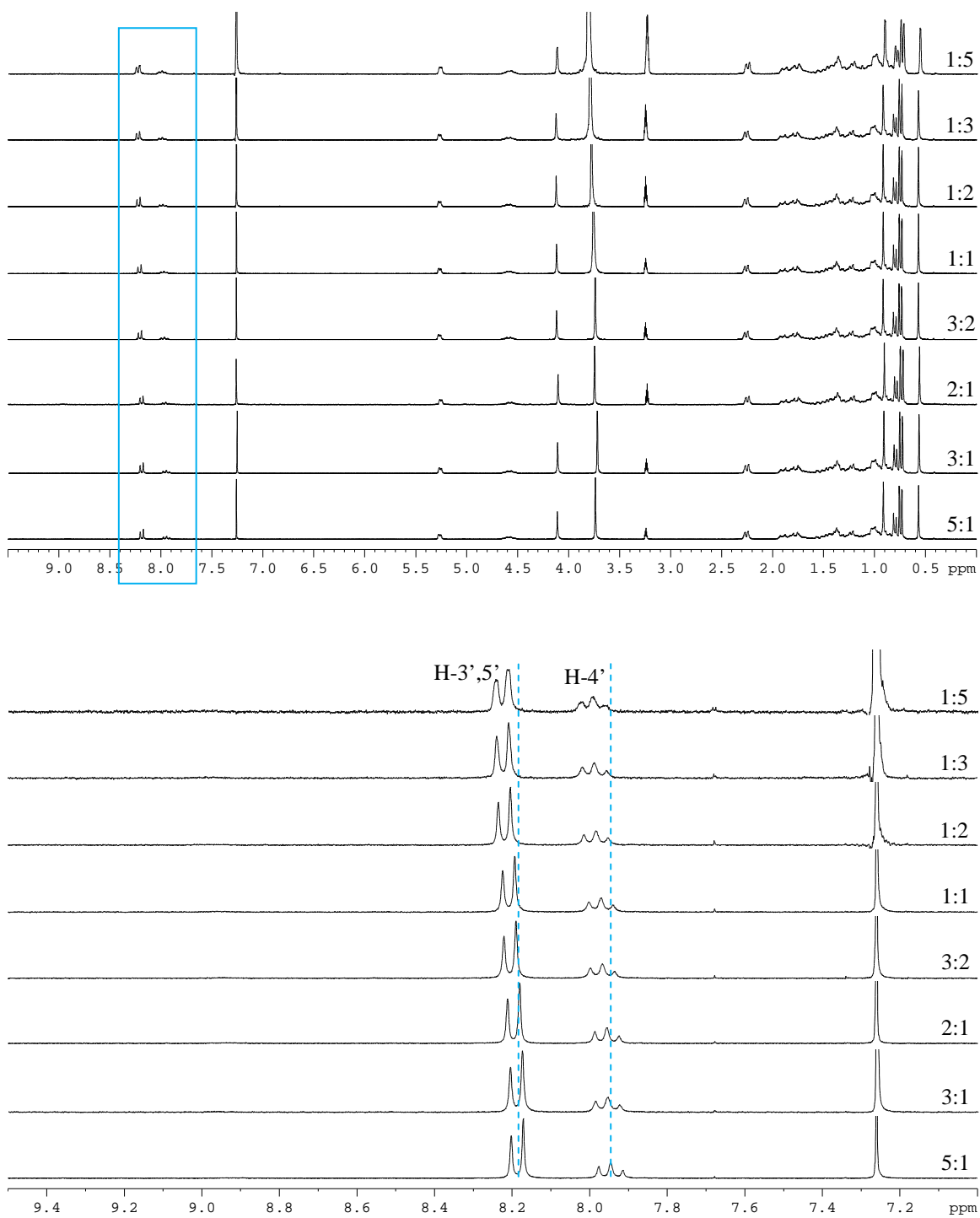


Fig. S6 ¹H NMR for Job plot of 1+Zn(II).

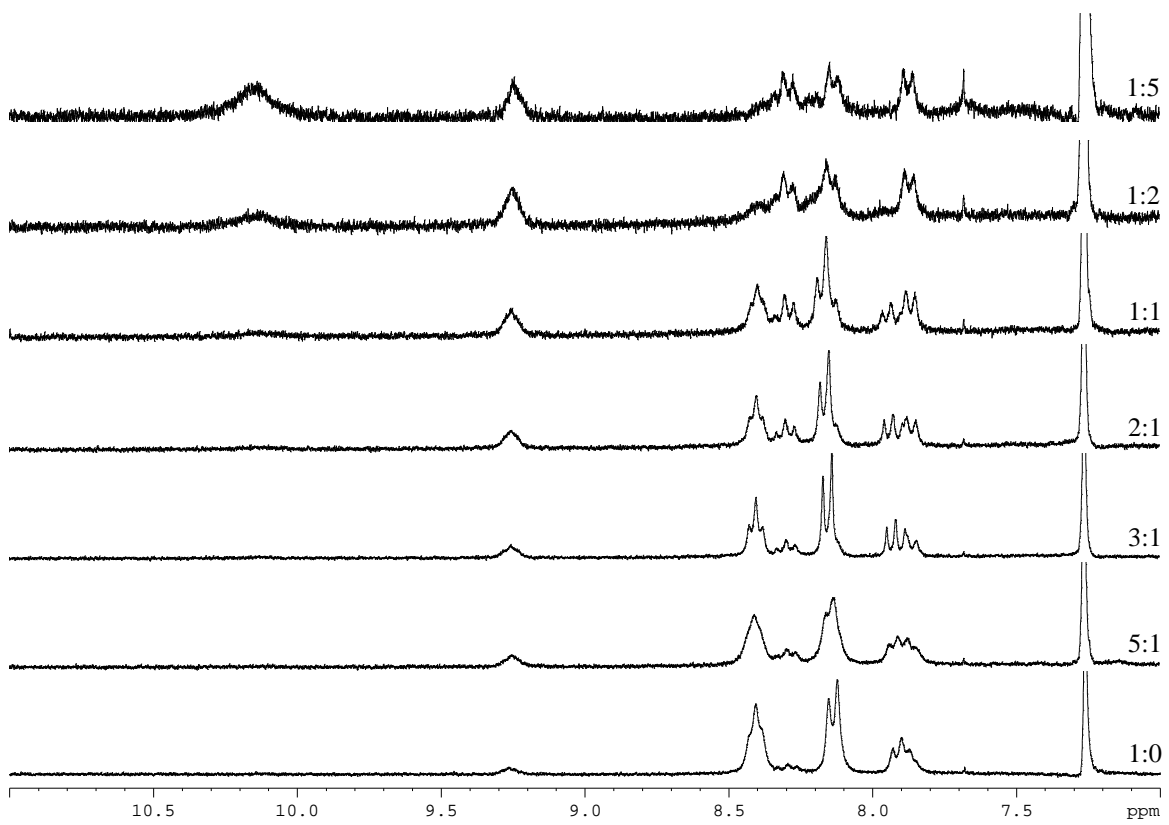
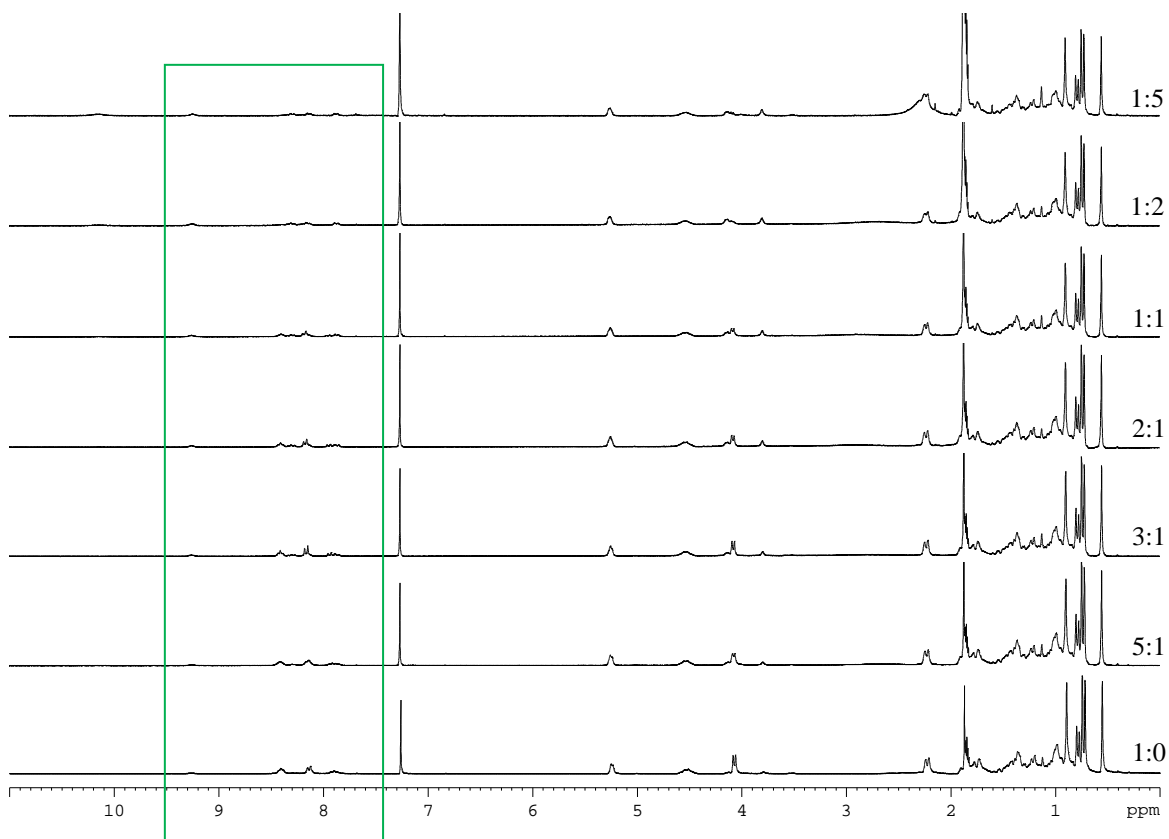
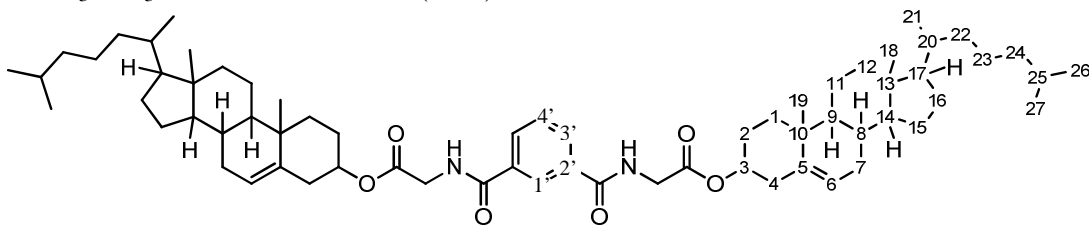


Fig. S7 ^1H NMR for Job plot of **1**+Pd(II).

Table S1 ^{13}C NMR chemical shifts of gelator **1** and **2**, and their metal complexes in a $\text{CDCl}_3\text{-CD}_3\text{OD}$ solvent mixture (12:1).



^{13}C NMR	1	1+Ag(I)	1+Zn(II)	2	2+Ag(I)	2+Zn(II)
C=O (Gly)	169.51	169.58	169.38	169.55	169.60	169.54
C=O	163.97	164.37	163.94	167.27	167.45	167.24
C-2'	148.18	148.17	147.73	133.85	133.86	133.86
C-5	139.23	139.45	139.21	139.23	139.58	139.23
C-4'	138.92	139.75	139.21	128.93	128.95	128.92
C-3'	125.11	125.23	125.18	130.61	130.59	130.61
C-1'	-	-	-	125.44	125.40	125.43
C-6	122.91	122.28	122.91	122.88	122.45	122.88
C-3	75.67	75.77	75.71	75.57	75.63	75.56
C-14	56.62	56.61	56.61	56.61	56.60	56.61
C-17	56.10	56.10	56.09	56.08	56.08	56.08
C-9	49.97	50.04	49.96	49.96	50.01	49.95
C-13	42.23	42.23	42.22	42.22	42.22	42.22
C-Gly	41.45	41.60	41.56	41.88	41.91	41.88
C-12	39.64	39.63	39.64	39.64	39.62	39.64
C-24	39.41	39.41	39.40	39.41	39.40	39.40
C-4	37.89	37.85	37.87	37.88	37.85	37.88
C-1	36.85	36.90	36.83	36.82	36.87	36.82
C-10	36.48	36.56	36.47	36.47	36.53	36.48
C-22	36.09	36.09	36.09	36.09	36.09	36.09
C-20	35.69	35.69	35.68	35.68	35.67	35.68
C-8	31.81	31.81	31.80	31.79	31.79	31.79
C-7	31.75	31.73	31.74	31.75	31.73	31.75
C-16	28.09	28.09	28.08	28.09	28.08	28.09
C-25	27.88	27.89	27.88	27.88	27.88	27.88
C-2	27.58	27.52	27.56	27.58	27.54	27.58
C-15	24.16	24.15	24.16	24.15	24.14	24.15
C-23	23.75	23.76	23.74	23.73	23.73	23.73
C-26	22.64	22.64	22.63	22.63	22.63	22.63
C-27	22.39	22.40	22.39	22.39	22.39	22.38
C-11	20.95	20.95	20.94	20.93	20.93	20.93
C-19	19.15	19.18	19.14	19.13	19.16	19.13
C-21	18.59	18.59	18.59	18.58	18.58	18.58
C-18	11.73	11.73	11.72	11.72	11.72	11.72

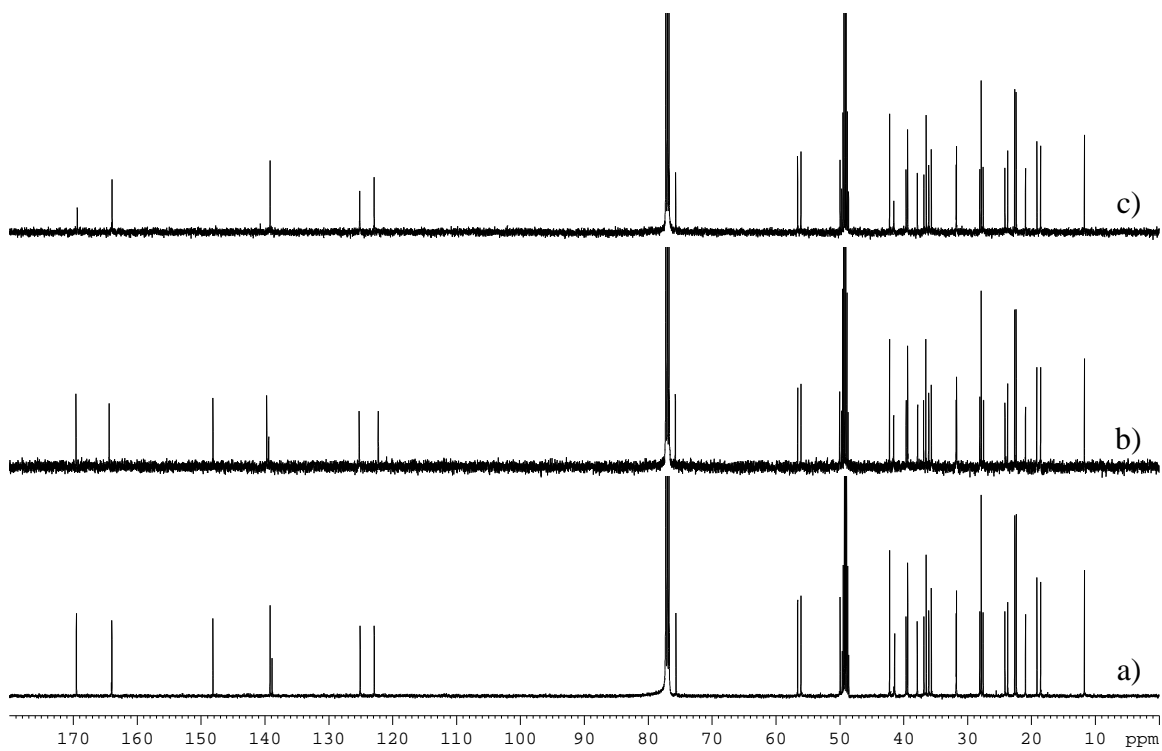


Fig. S8 ^{13}C NMR spectra of (a) **1**, (b) **1**+Ag(I), and (c) **1**+Zn(II).

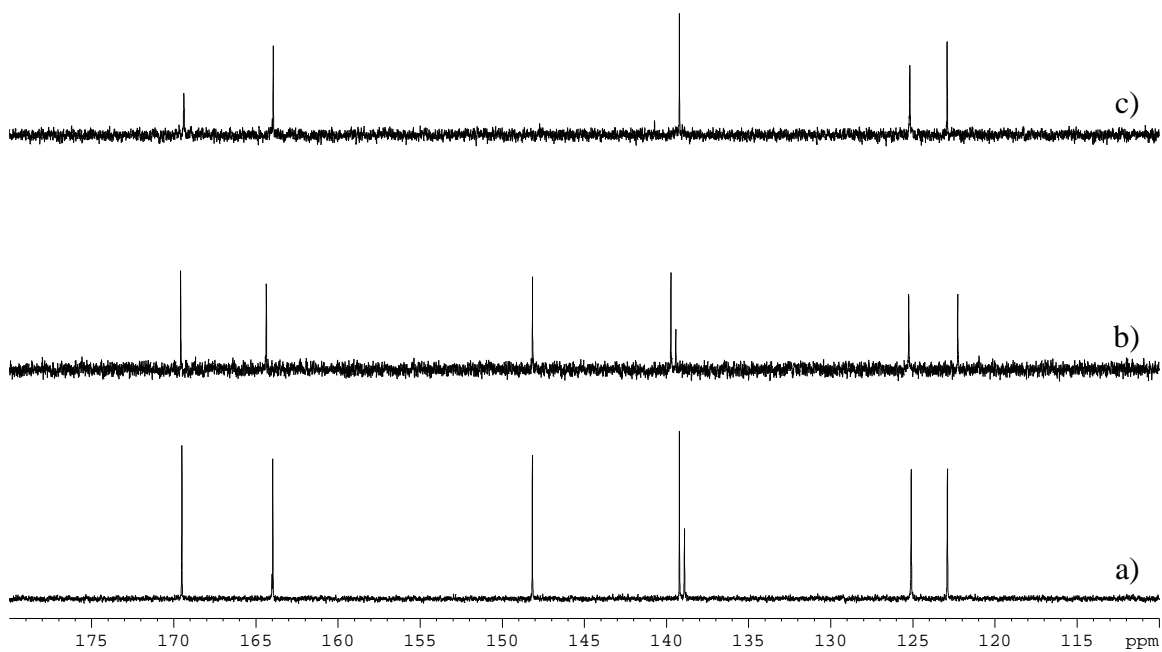
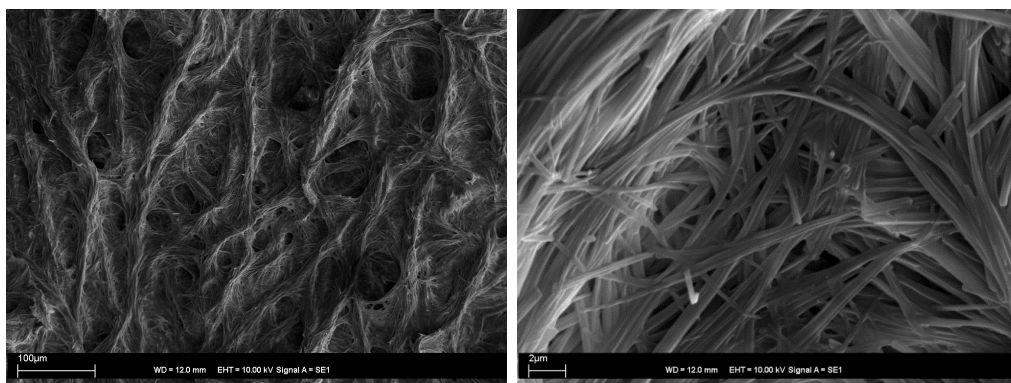


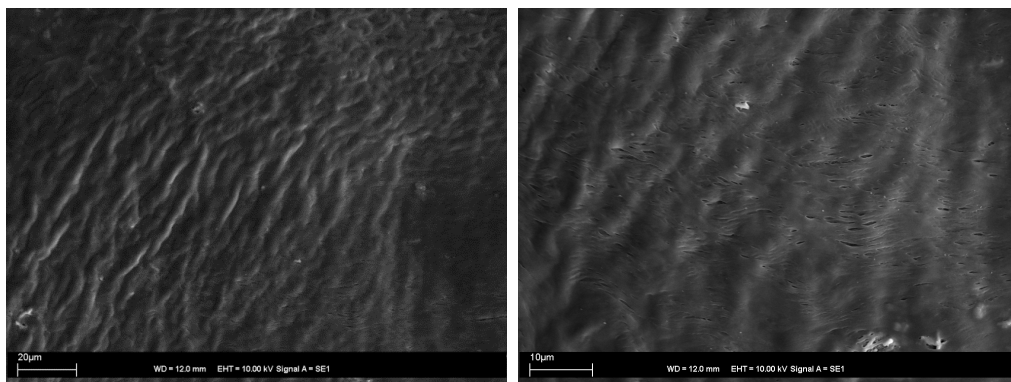
Fig. S9 ^{13}C NMR spectra of (a) **2**, (b) **2**+Ag(I), and (c) **2**+Zn(II).

SEM measurement

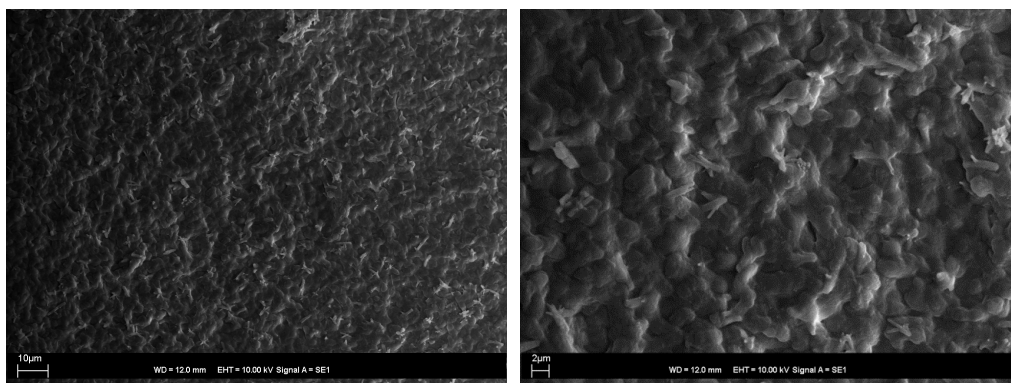
Scanning electron micrographs of xerogels were taken on a Bruker Quantax400 EDS microscope equipped with a digital camera. The samples of the xerogels were prepared by placing a hot, clear solution of the gelator on carbon tape over a sample stub. The samples were dried at room temperature and then sputter coated with a thin layer of gold in a JEOL Fine Coat Ion Sputter JFC-1100.



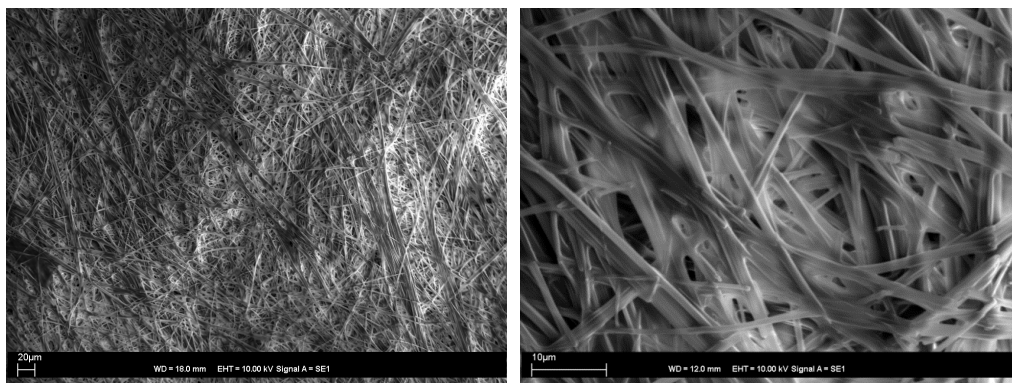
SEM images of xerogel obtained from the gel of **1** in pentan-1-ol (2% w/v).



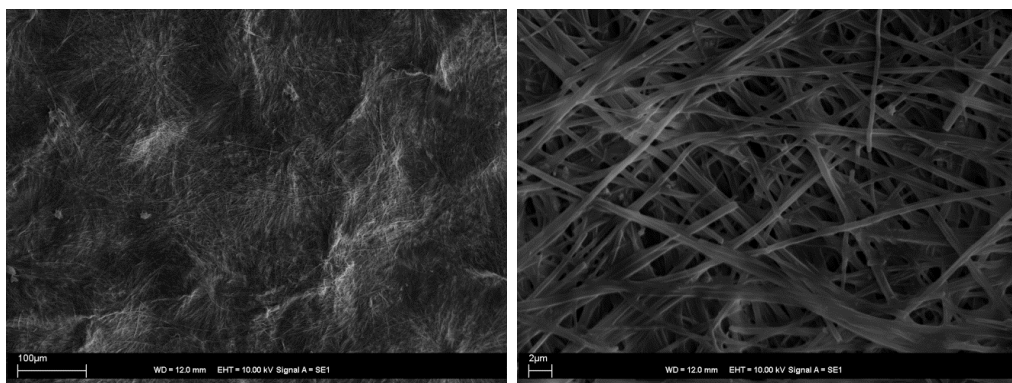
SEM images of xerogel obtained from the gel of **1**+Ag(I) in pentan-1-ol (2% w/v).



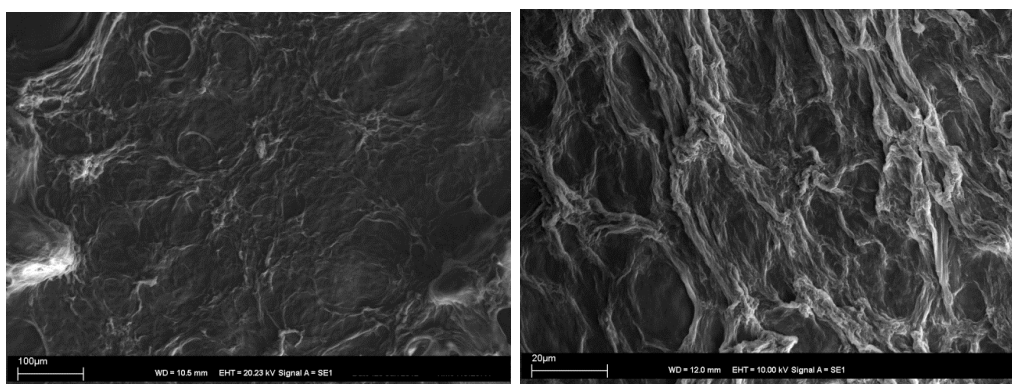
SEM images of xerogel obtained from the gel of **1**+Zn(II) in pentan-1-ol (2% w/v).



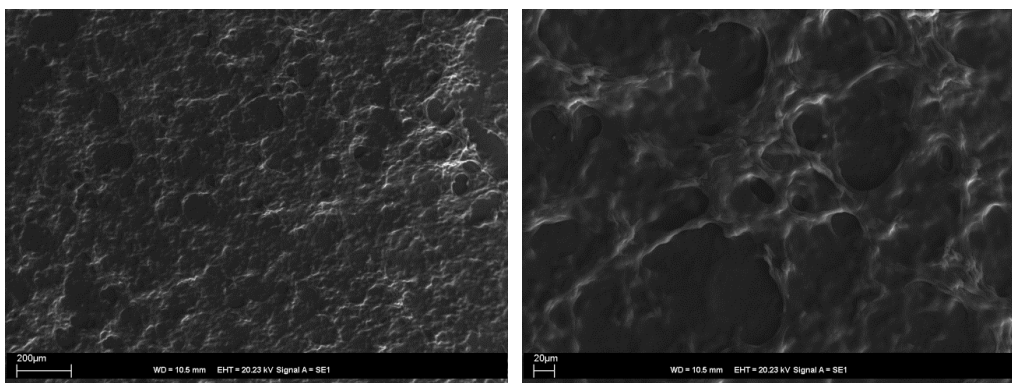
SEM images of xerogel obtained from the gel of **2** in pentan-1-ol (2% w/v).



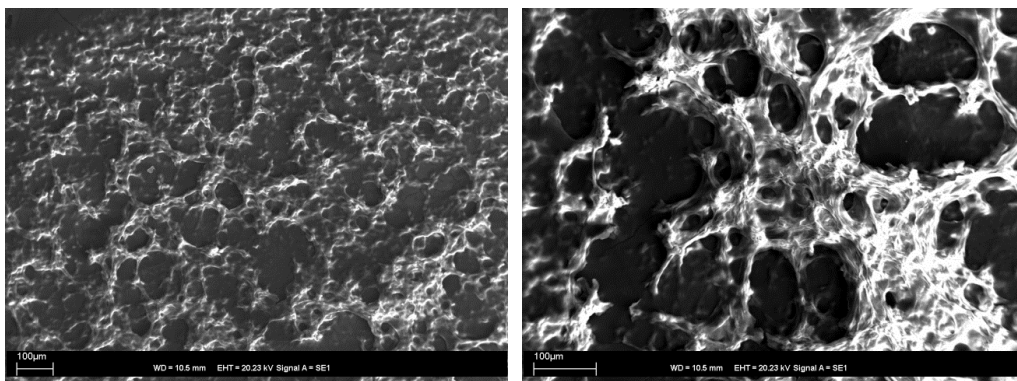
SEM images of xerogel obtained from the gel of **2**+Zn(II) in pentan-1-ol (2% w/v).



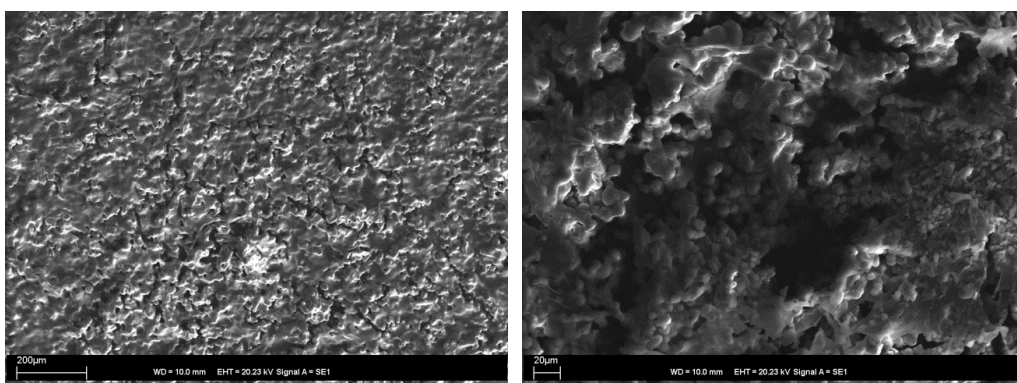
SEM images of xerogel obtained from the gel of **1** in DMF (1% w/v).



SEM images of xerogel obtained from the gel of **1**+Ag(I) in DMF (1% w/v).



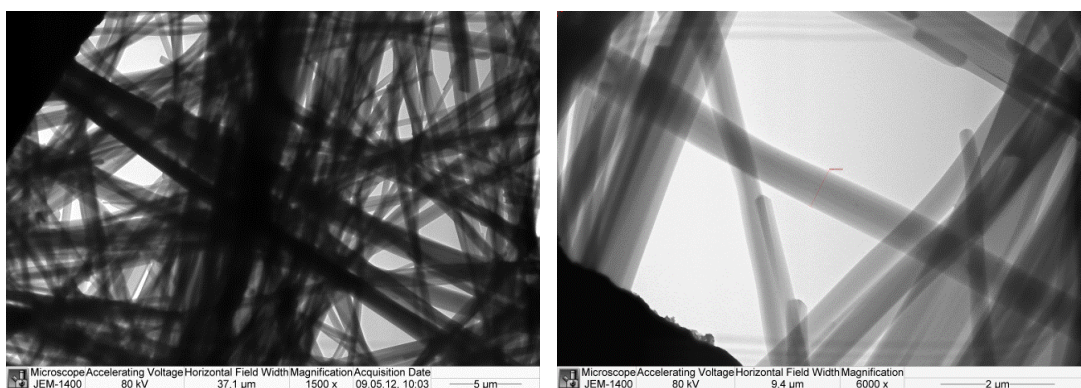
SEM images of xerogel obtained from the gel of **1**+Zn(II) in DMF (1% w/v).



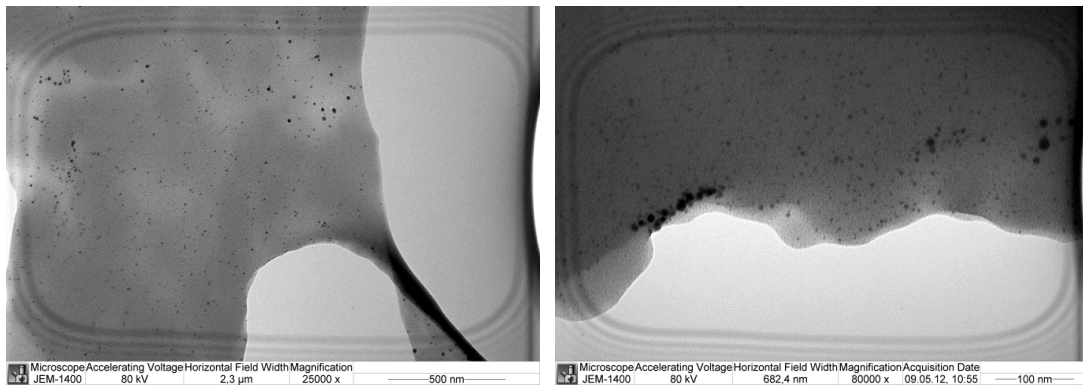
SEM images of xerogel obtained from the gel of **1**+Pd(II) in DMF (1% w/v).

TEM measurement

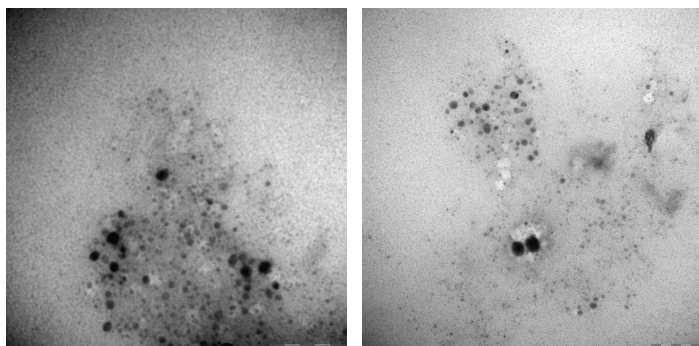
Transition electron micrographs of pentan-1-ol xerogels were acquired using a JEOL JEM-1400 Electron Microscope. The samples of the xerogels were prepared by placing a gel or a hot clear solution of the gelator on a grid and were dried at room temperature.



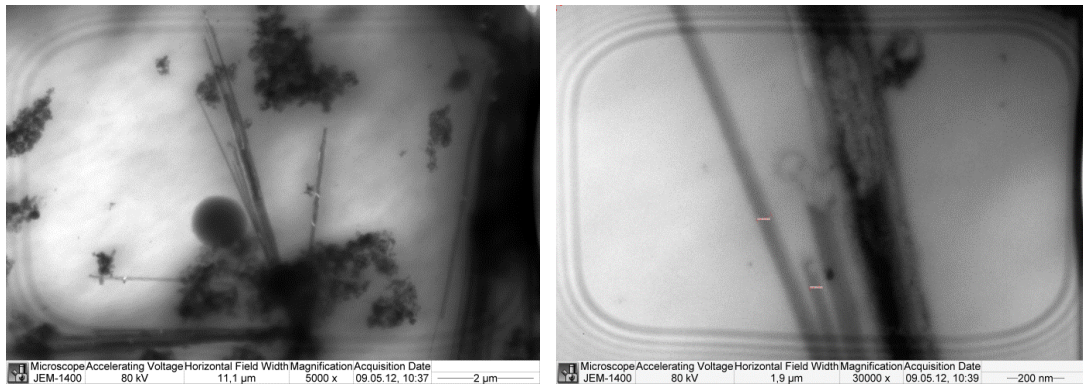
TEM images of xerogel obtained from the gel of **1** in pentan-1-ol (2% w/v).



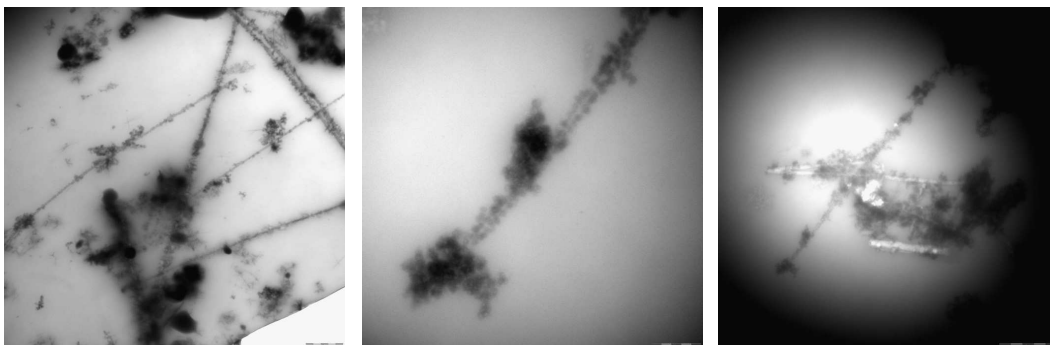
TEM images of xerogel obtained from the gel of **1**+Ag(I) in pentan-1-ol (2% w/v).



TEM images of xerogel obtained from the freshly prepared hot solution of **1**+Ag(I) in pentan-1-ol (2% w/v).



TEM images of xerogel obtained from the gel of **1**+Zn(II) in pentan-1-ol (2% w/v).



TEM images of xerogel obtained from the freshly prepared hot solution of **1**+Zn(II) in pentan-1-ol (2% w/v).

Analysis of silver nanoparticles obtained from the gel of **1**+Ag(I) in pentan-1-ol

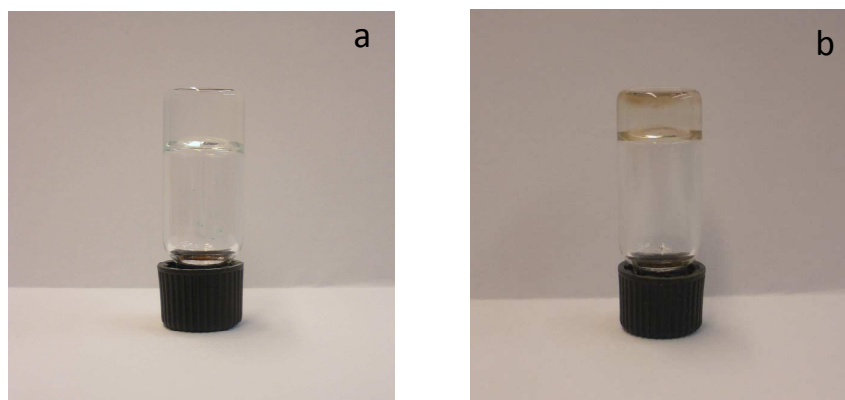


Fig. S10 Photographs of (a) freshly prepared gel of **1**+Ag(I) in pentan-1-ol, and (b) gel of **1**+Ag(I) in pentan-1-ol which was exposed to the day light for several weeks.

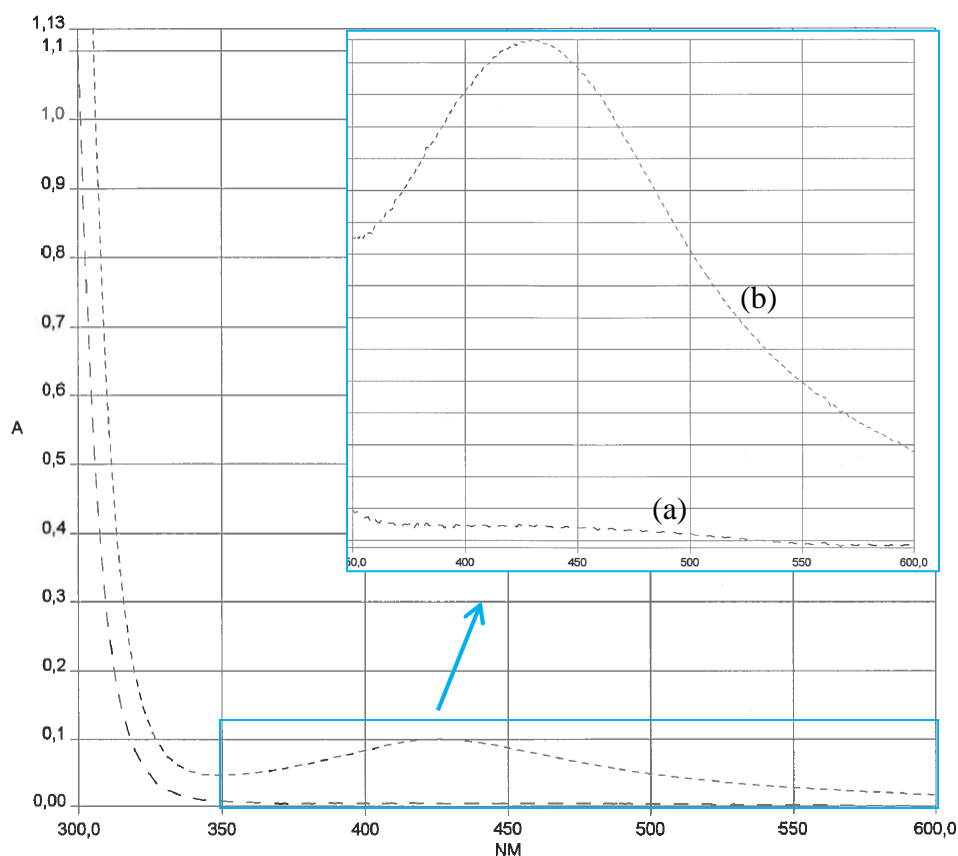


Fig. S11 UV-VIS spectrum of (a) freshly prepared gel of **1**+Ag(I) in pentan-1-ol, (b) gel of **1**+Ag(I) in pentan-1-ol which was exposed to the day light for three weeks.

Note: The same amounts of the gel samples were dissolved in CHCl_3 and then measured.

Variable Temperature (VT) ^1H NMR measurements

VT ^1H NMR spectra were recorded with a Bruker Avance DRX 500 NMR spectrometer equipped with a 5 mm diameter broad band inverse probe head working at 500.13 MHz for ^1H . Samples were prepared directly in an NMR tube; a weighed amount of the gelator was dissolved upon heating in 0.6 mL of $\text{DMF-}d_7$, and gel samples were stabilized overnight. The VT ^1H NMR experiment was conducted by heating the sample at 10 °C in each step. The sample was allowed to stabilize for 5 min at each temperature before acquiring the spectrum.

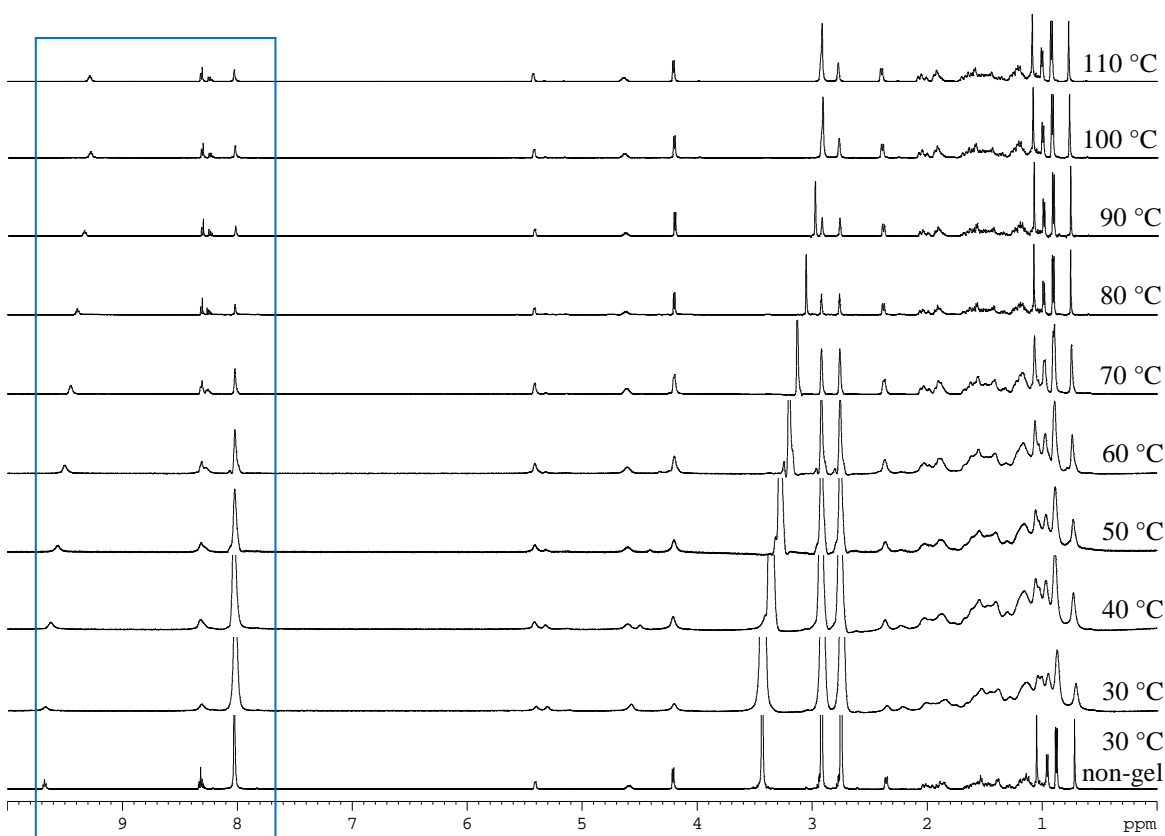


Fig. S12 ^1H NMR spectra of **1** in $\text{DMF-}d_7$ at non-gelling concentration, and as a $\text{DMF-}d_7$ gel (2% w/v) at different temperatures (30-110 °C).

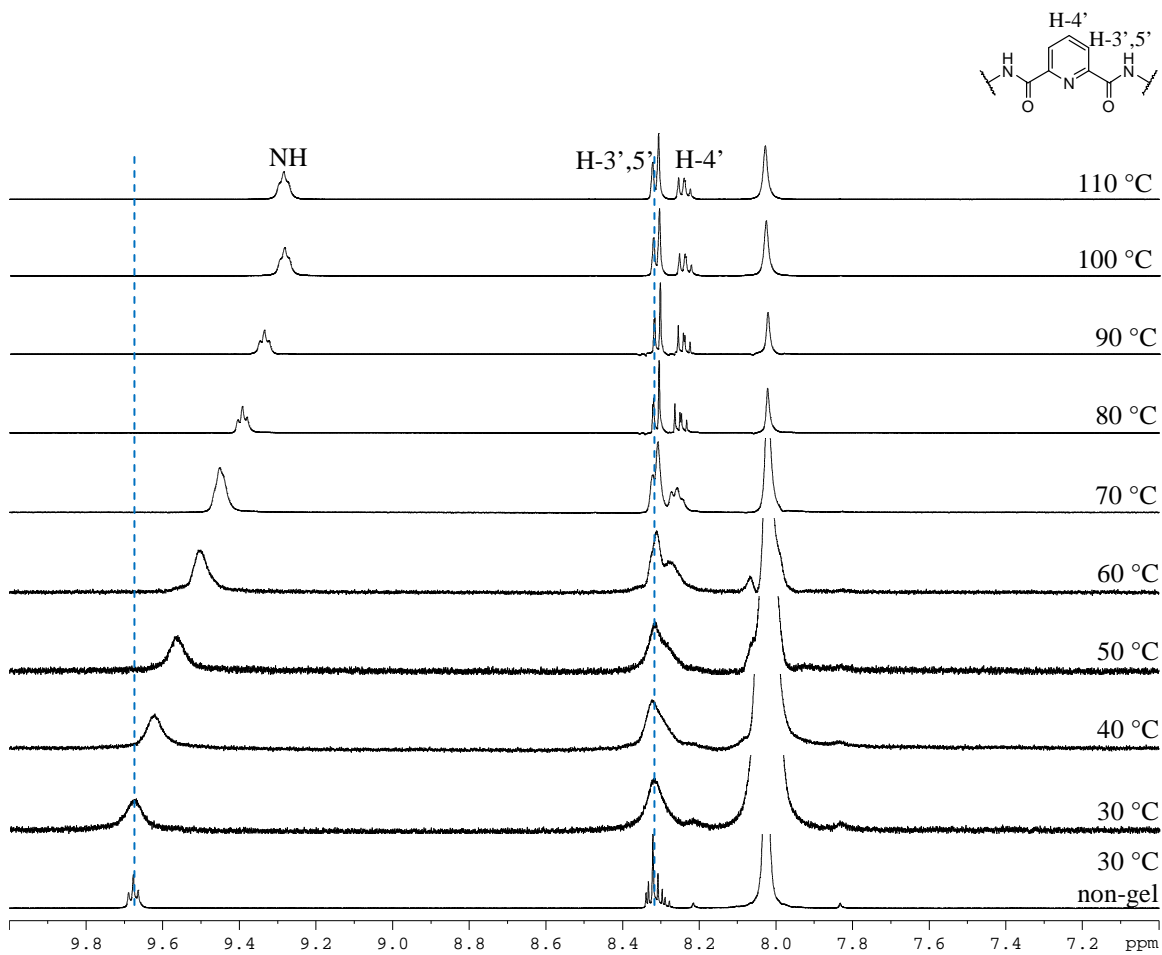


Fig. S13 ¹H NMR spectra of **1** in DMF-*d*₇ at non-gelling concentration, and as a DMF-*d*₇ gel (2% w/v) at different temperatures (30-110 °C).

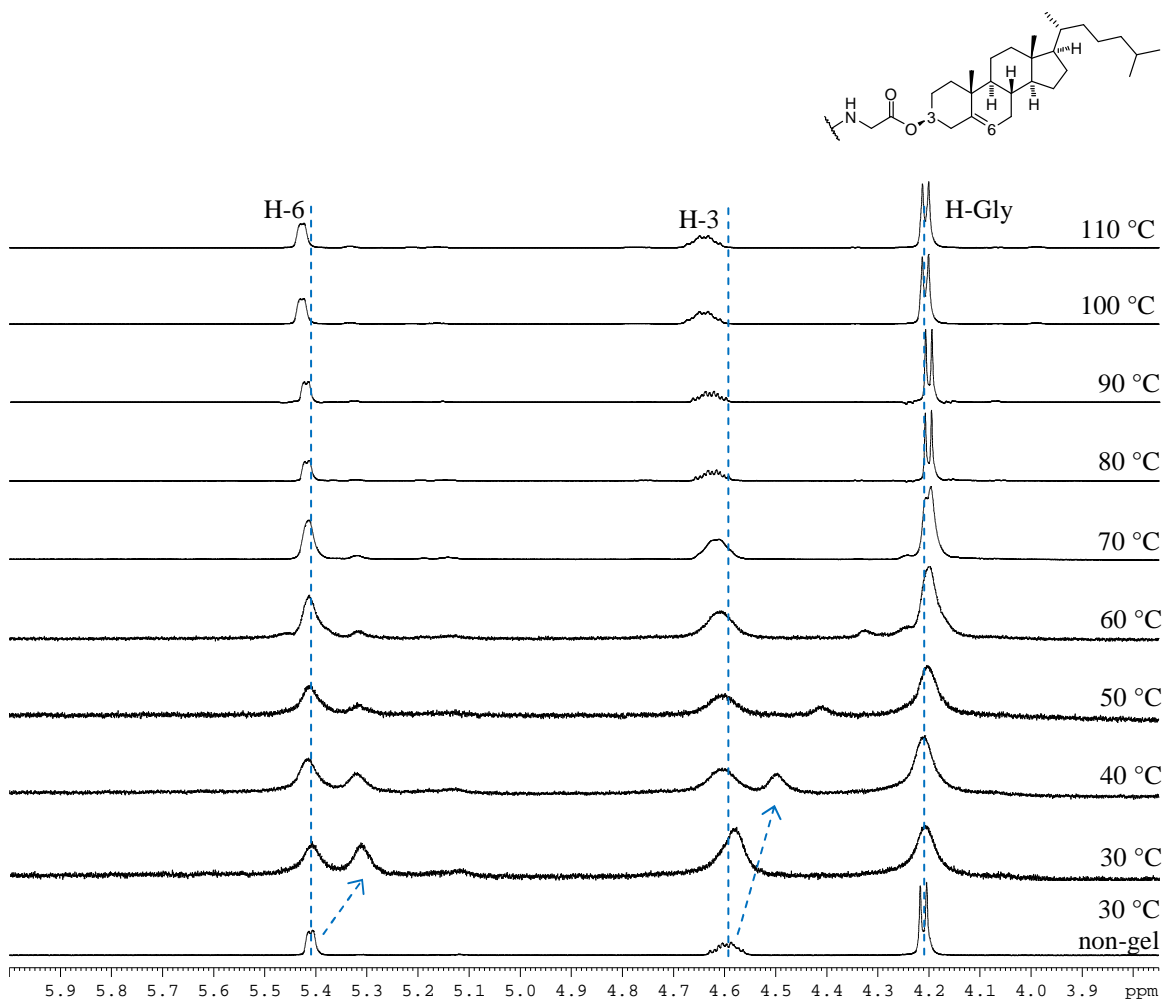


Fig. S14 ^1H NMR spectra of **1** in $\text{DMF-}d_7$ at non-gelling concentration, and as a $\text{DMF-}d_7$ gel (2% w/v) at different temperatures (30-110 °C).

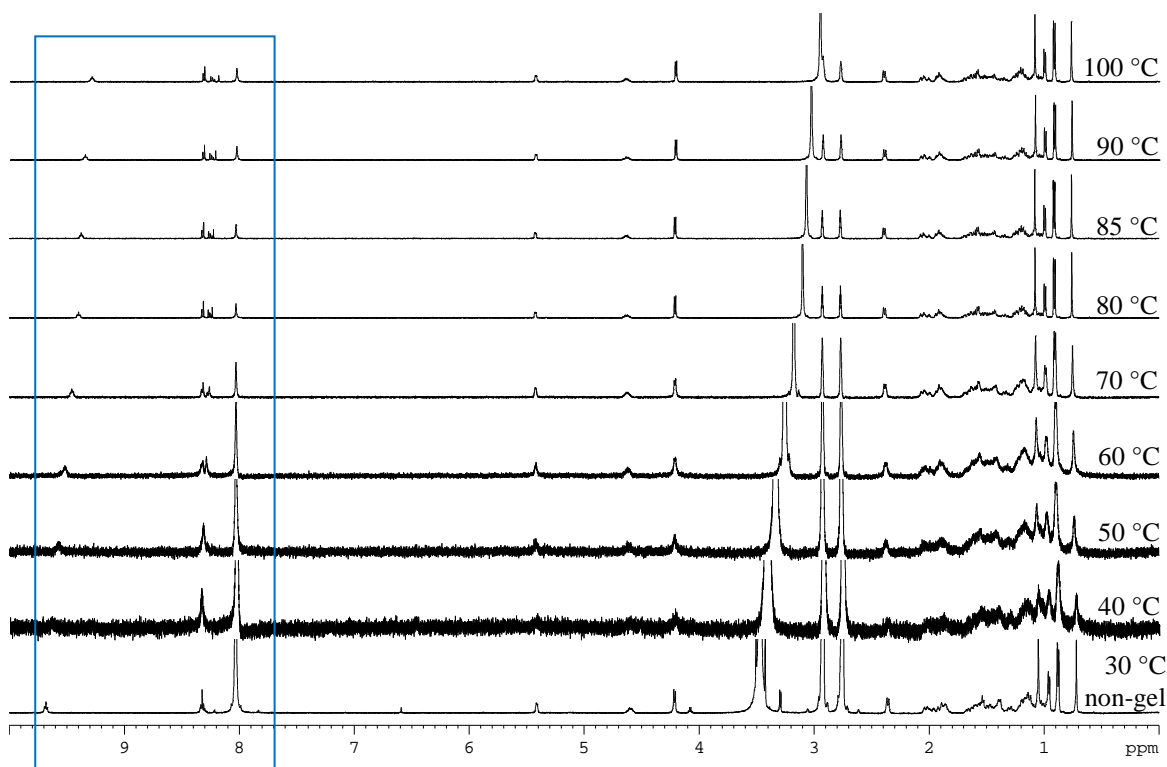


Fig. S15 ^1H NMR spectra of **1**+Zn(II) in $\text{DMF-}d_7$ at non-gelling concentration, and as a $\text{DMF-}d_7$ gel (2% w/v) at different temperatures (40-100 °C).

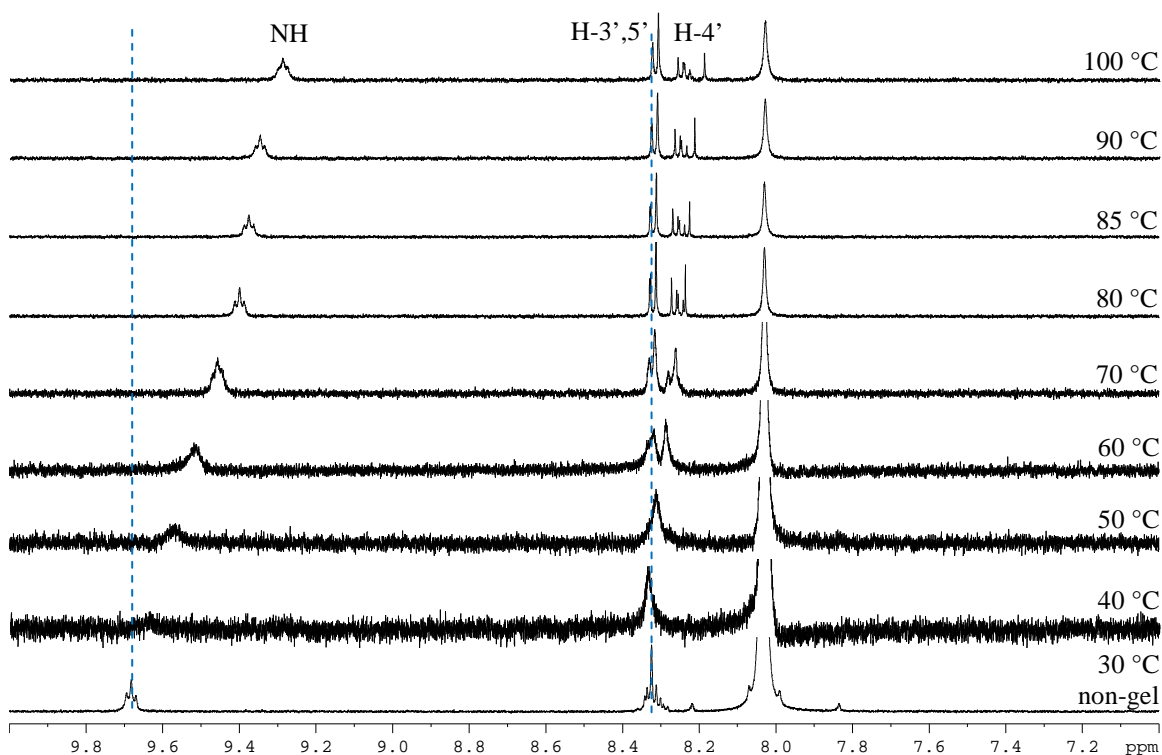


Fig. S16 ^1H NMR spectra of **1**+Zn(II) in $\text{DMF-}d_7$ at non-gelling concentration, and as a $\text{DMF-}d_7$ gel (2% w/v) at different temperatures (40-100 °C).

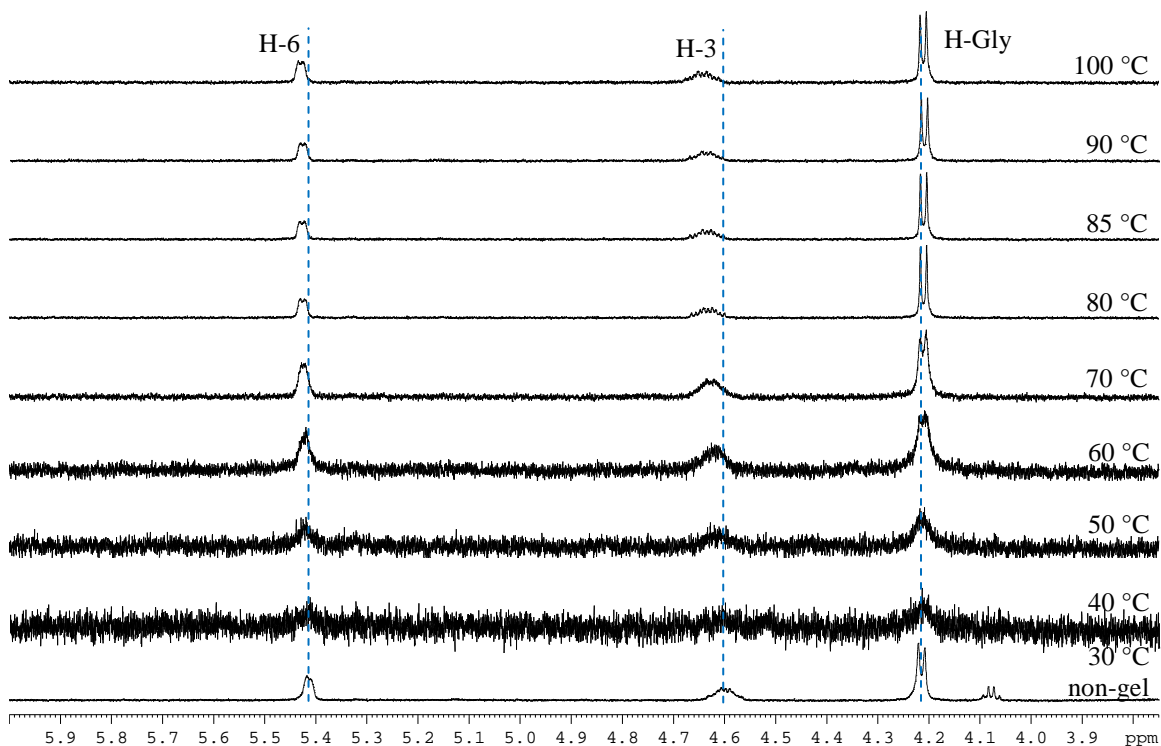


Fig. S17 ^1H NMR spectra of **1**+Zn(II) in $\text{DMF-}d_7$ at non-gelling concentration, and as a $\text{DMF-}d_7$ gel (2% w/v) at different temperatures (40-100 °C).

Solid-state NMR measurements

The ^{13}C and ^{15}N CPMAS NMR spectra were recorded on a Bruker AV 400 spectrometer equipped with a 4 mm standard bore CPMAS probehead whose X channel was tuned to 100.62 MHz for ^{13}C and 40.55 MHz for ^{15}N , respectively. The other channel was tuned to 400.13 MHz for broad band ^1H decoupling. The dried and finely powdered samples were packed in the ZrO_2 rotor closed with Kel-F cap and spun at 10 kHz. The ^{13}C CPMAS NMR was carried out for all samples under Hartmann–Hahn conditions with TPPM decoupling. The $p/2$ pulse for proton and carbons were found to be 4.2 ms and 5 ms at power levels of -4.6 dB and -0.8 dB, respectively. The experiments were conducted at a contact time of 2 ms. A total of 20,000 scans were recorded with 5 s recycle delay for each sample. All free induction decays (FIDs) were processed by exponential apodization function with line broadening of 20–30 Hz prior to FT. All ^{13}C CPMAS chemical shifts are referenced to the resonances of a glycine (C=O, 176.03 ppm) standard measured prior to the sample itself.

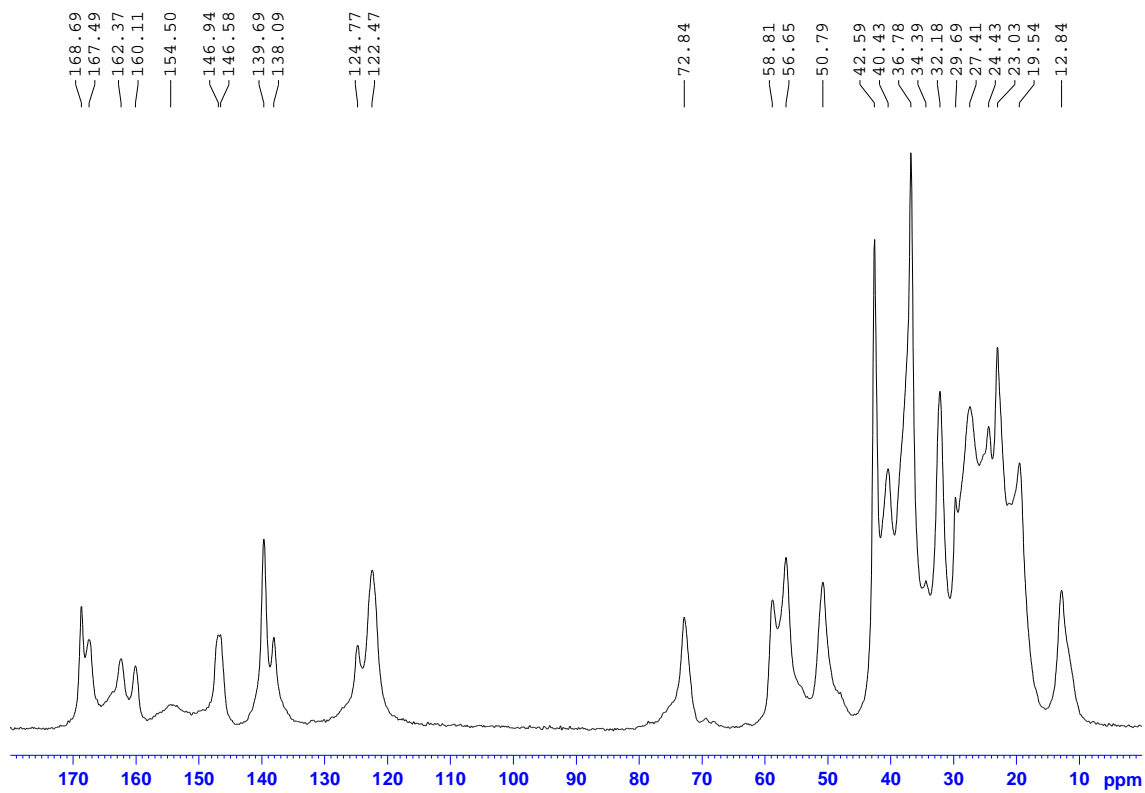


Fig. S18 ^{13}C CPMAS NMR spectrum of **1** (solid from chloroform).

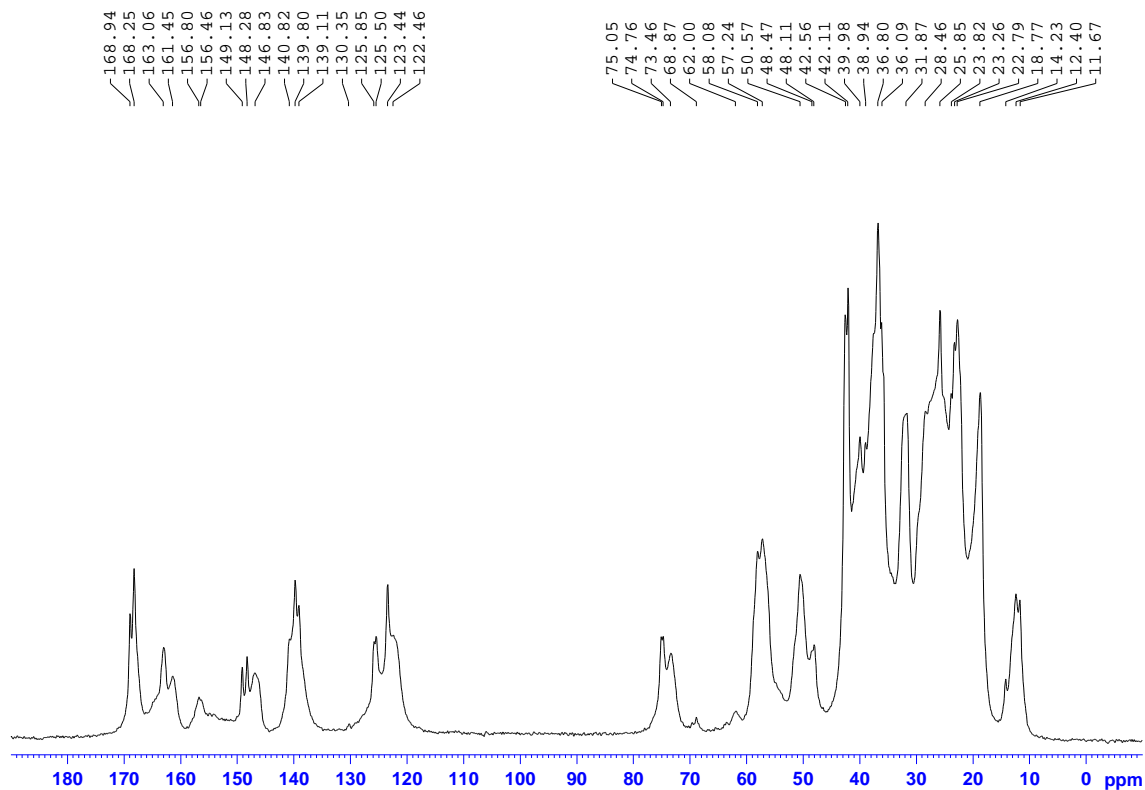


Fig. S19 ^{13}C CPMAS NMR spectrum of **1** (xerogel from pentan-1-ol).

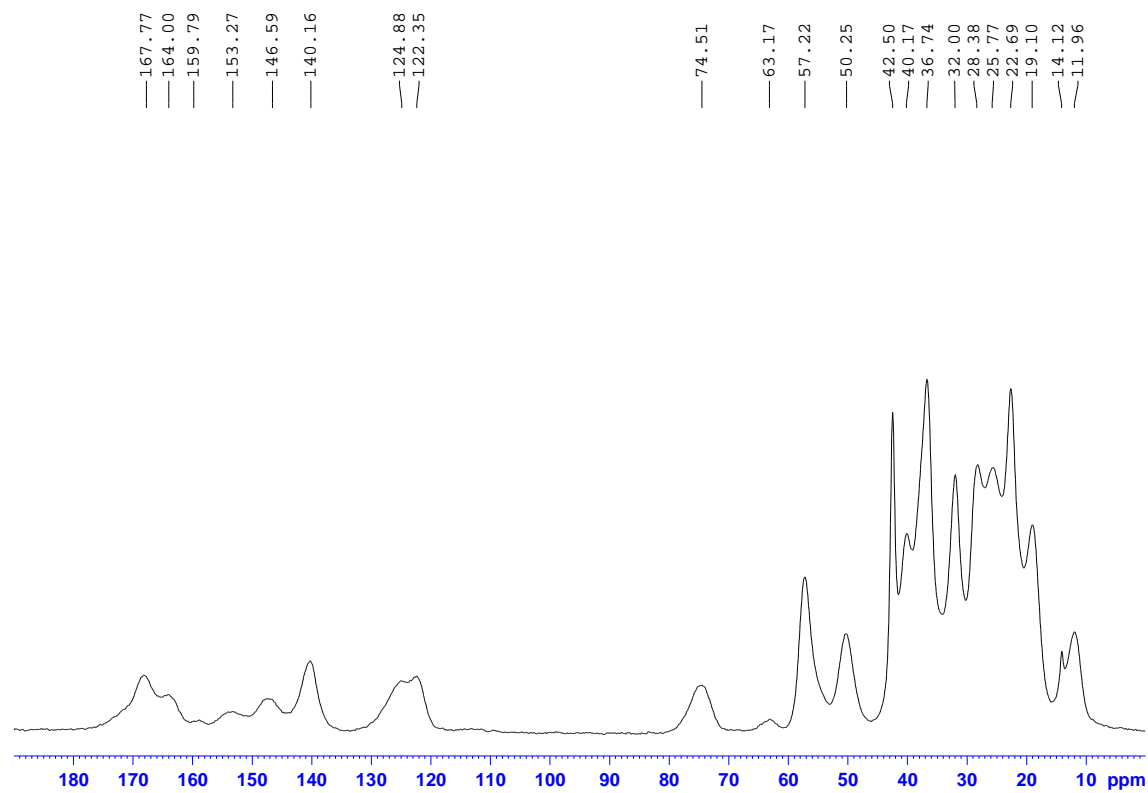


Fig. S20 ^{13}C CPMAS NMR spectrum of **1**+Ag(I) (xerogel from pentan-1-ol).

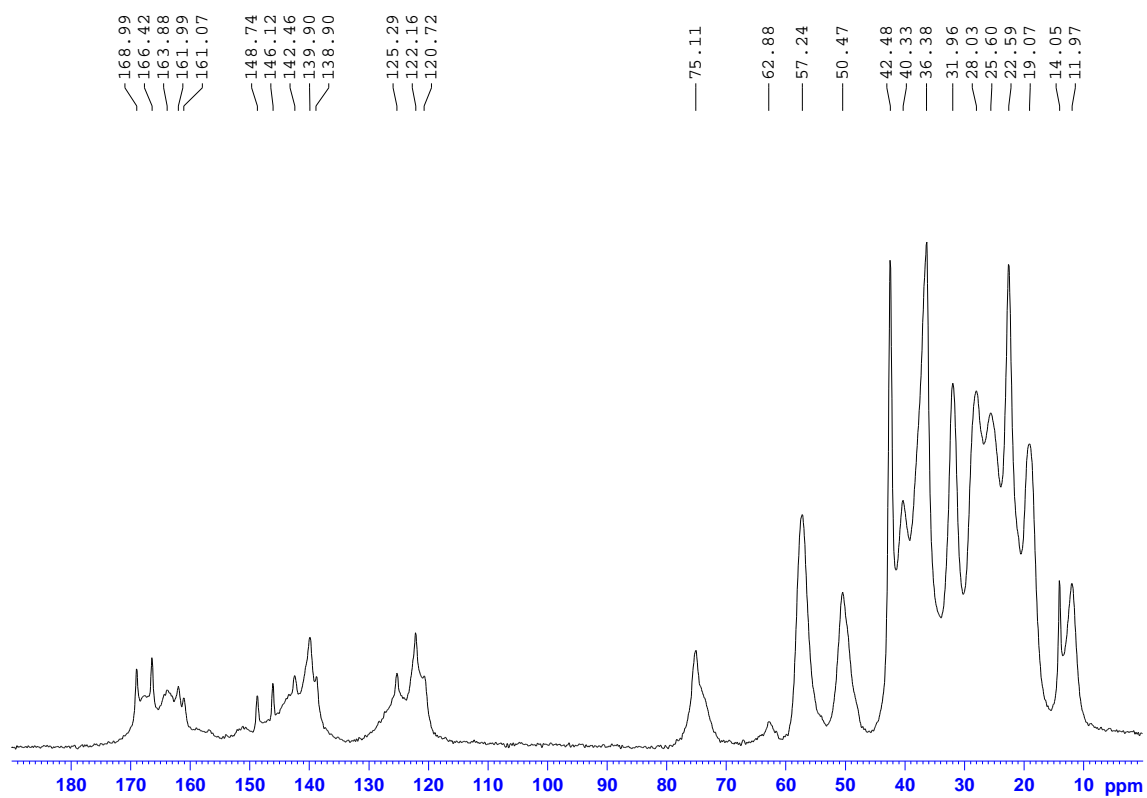


Fig. S21 ^{13}C CPMAS NMR spectrum of **1**+Zn(II) (xerogel from pentan-1-ol).

Powder X-ray diffraction analysis

The X-ray powder diffraction data of xerogels of compound **1** were measured with PANalytical X'Pert PRO diffractometer in Bragg–Brentano geometry using Johansson monochromatized Cu $K_{\alpha 1}$ radiation (1.5406 Å; 45 kV, 30 mA). As received fine powder samples were prepared on a silicon-made zero-background holder using petrolatum jelly as an adhesive. The data acquisition was made from a spinning sample by X'Celerator detector in the 2θ range of 1–50° with a step size of 0.017°, counting times of 480 s per step. The acquired data was processed and analysed using X'Pert HighScore Plus v. 2.2d software package.

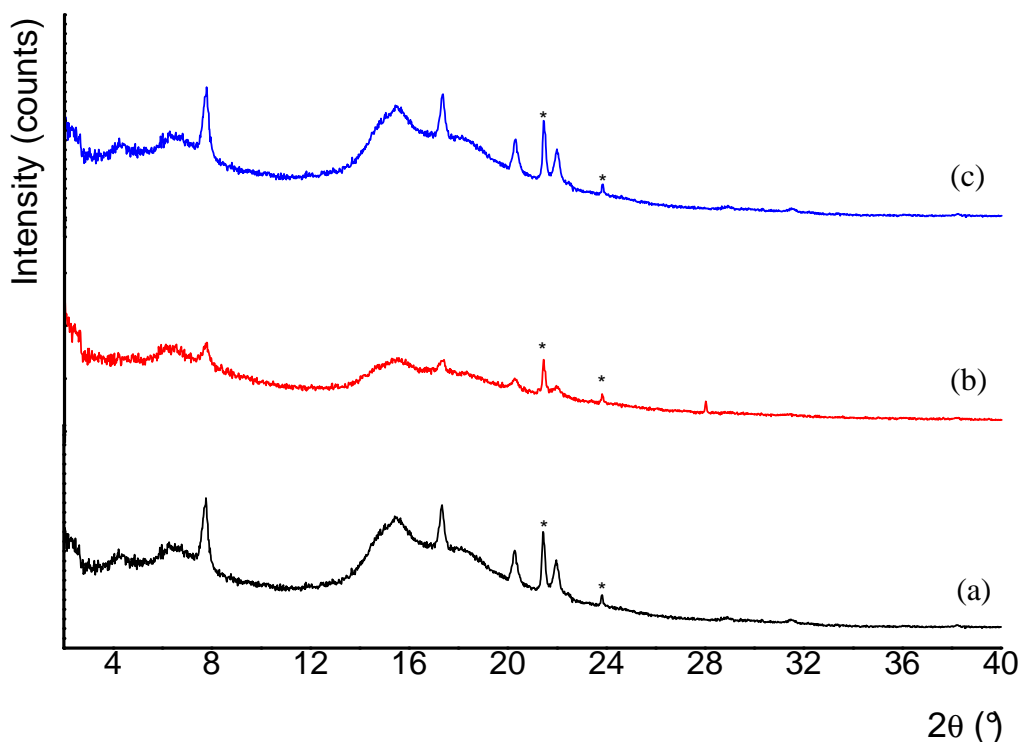


Fig. S22 Experimental powder diffraction patterns of (a) xerogel of **1** from DMF, (b) xerogel of **1**+Ag(I) from DMF, and (c) xerogel of **1**+Zn(II) from DMF.

Note: * indicates diffraction peaks originating from petrolatum jelly used as an adhesive.

Single-crystal diffraction analysis

The structural data for gelator **1** crystallized from DMF were collected at 150.0 ± 0.1 °C (Oxford Cryostream) with Agilent Supernova dual wavelength diffractometer, using micro-focus X-ray source and multilayer optics monochromatized $\text{CuK}\alpha$ radiation ($\lambda = 1.54184$ Å; 50 kV, 0.8 mA). The data collection, reduction, multi-scan and analytical face-index based absorption corrections were made by program CrysAlis^{Pro}.¹ The crystal structure was solved by Superflip² implemented in program Olex2³ (v 1.2) and refined (ShelXH)⁴ on F^2 by full matrix least squares techniques using anisotropic displacement parameters for all non-hydrogen atoms. Hydrogen atoms were calculated to their positions as riding atoms using isotropic displacement parameters (1.2 – 1.5 times higher than the attached host atom). Restrained disorder models were constructed for one of the aliphatic terminal groups (isopropyl end) as well as for two DMF solvent molecules. The program Mercury⁵ was used for depicting the crystal structures. The above normal residual electron density (isolated q-peak with $1.38 \text{ e } \text{Å}^{-3}$) is observed about 1.4 Å distance from carbonyl group (O13), and is most likely caused by the imperfections of the crystal used in the measurement, as no reasonable chemical explanation for the observed q-peak nor twin laws (PLATON)⁶ for the dataset could be found.

References:

1. CrysAlis^{Pro}, version 1.171.35.21, Agilent Technologies, Oxford, **2012**.
2. C. Baerlocher, L. McCusker and L. Palatinus, Charge flipping combined with histogram matching to solve complex crystal structures from powder diffraction data, *Z. Kristallogr.* **222**, **2007**, 47–53.
3. O.V. Dolomanov, L.J. Bourhis, R.J Gildea, J.A.K Howard, H. Puschmann, OLEX2: a complete structure solution, refinement and analysis program, *J. Appl. Cryst.* **42**, **2009**, 339-341.
4. G.M. Sheldrick, *Acta Crystallogr.*, Sect. A **64**, **2008**, 112-122.
5. C.F. Macrae, I.J. Bruno, J.A. Chisholm, P.R. Edgington, P. McCabe, E. Pidcock, L. Rodriguez-Monge, R. Taylor, J. van de Streek, P.A. Wood, Mercury CSD 2.0 - new features for the visualization and investigation of crystal structures. *J. Appl. Cryst.* **41**, **2008**, 466-470.
6. A. L. Spek, Single-crystal structure validation with the program PLATON, *J. Appl. Cryst.* **36**, **2003**, 7-13.

Description of the single crystal structure of gelator 1

Small, fragile and plate-like crystals (Fig. S23) of gelator **1** were obtained by very slow evaporation of the solvent from the DMF gel of **1**+Ag(I). Several of these crystals were subjected to the single crystal X-ray diffraction analysis. Nearly all crystals were able to index to a triclinic crystal system with unit cell parameters shown in a Table S2. Generally, crystallographic quality of all crystals was rather low but structure analysis was still successfully made with two crystals. The chirality of the cholesteryl moiety is originally known and its chiral centers remained unchanged in the reactions yielding the gelator **1**. However, due to somewhat low quality dataset (merged $I/\sigma = \sim 8$) and lack of heavier elements having the adequate scattering power for anomalous scattering, reliable determination of the absolute configuration was unsuccessful, even though over 90% of all Friedel-pairs were measured with Cu radiation.

Based on the structure analysis, gelator **1** crystallizes as a DMF disolvate (**1**·DMF) in triclinic chiral space group *P*1. The asymmetric unit is consisted of two conformationally distinct gelator molecules and four DMF solvent molecules. The conformational difference of the gelator molecules is manifested by nearly 180° turn of the cholesteryl group in one of the gelator molecules. This causes cholesteryl groups on the adjacent gelator molecules to be face-to-face on their “belly” sides, whereas on the other side of the pyridyl core the cholesteryl groups of adjacent molecules are organized in parallel fashion, as can be seen in Figure S25. Moreover, one of the cholesteryl end groups show slight disorder having the outmost isopropyl end (atoms C72 – C74) being located over two positions with occupancies 0.7/0.3. On each gelator molecule, the two cholesteryl groups across the pyridyl core are tilted about 74° in relation to each other (Fig. S25).

The solvent molecules (DMF) are located in two separate infinite voids running along the *a*-axis. These voids are formed between columnary packed gelator molecules forming infinite molecular sheets also along *a*-axis (Fig. S26) Three of DMFs are in the same void whereas fourth one is isolated in the other void. Two of the DMFs have moderately strong H-bonds (bifurcated with average D···A distances of 2.93 – 3.1 Å, see Table S2) to the amide protons (one DMF for each crystallographically different gelator molecule) as can be seen in Figure S24. The other two DMFs are only loosely bound to their adjacent DMFs in the row and/or to close by gelator molecules via weak C–H···O=C hydrogen bonds (C–H of methyl or methylene) having average distances of ~3.4 – 3.6 Å for those having $\theta > 150^\circ$. The weak interactions are also manifested by the molecular disorder of both DMFs over two positions with site occupancies 0.5/0.5 and 0.7/0.3, respectively. The plausible π - π interaction between adjacent pyridyl groups is not observed in the structure due to DMFs residing between these units and no H-bonding is observed on pyridyl nitrogen (N1 and N75).

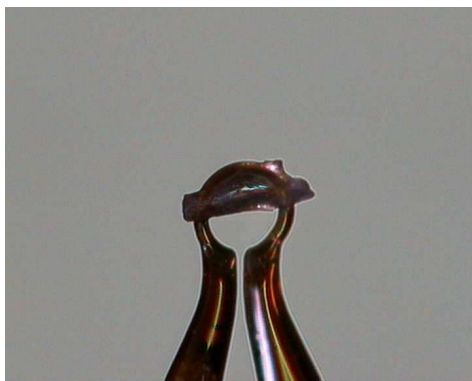


Fig. S23 Measured crystal mounted in 200 μm diameter MiTeGen loop.

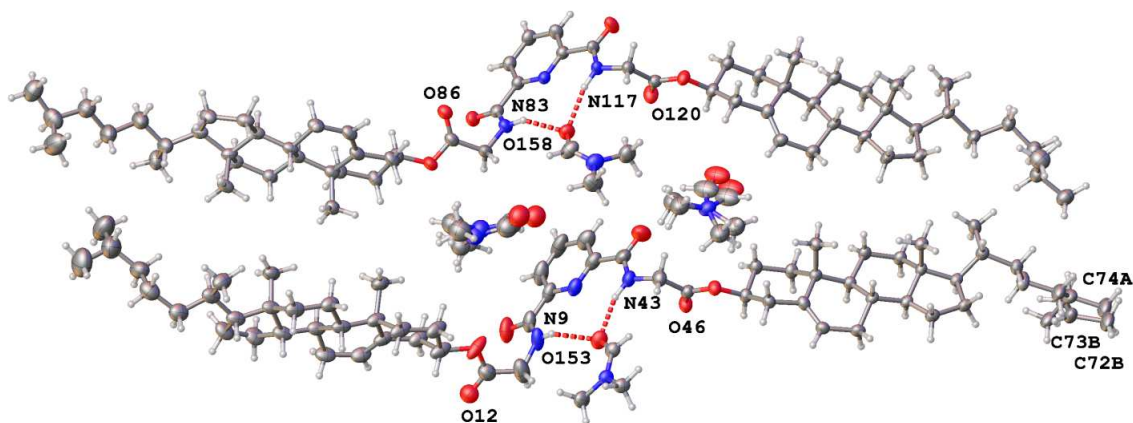


Fig. S24 Asymmetric unit, selected labeling and hydrogen bonding of gelator 1 DMF solvate. Thermal ellipsoids are at 50 % probability level.

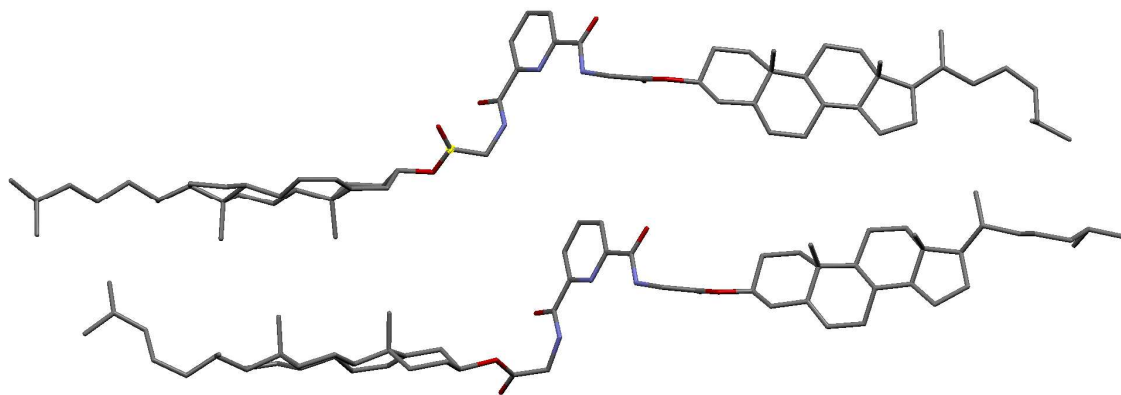


Fig. S25 View of conformational difference of the gelator molecules.

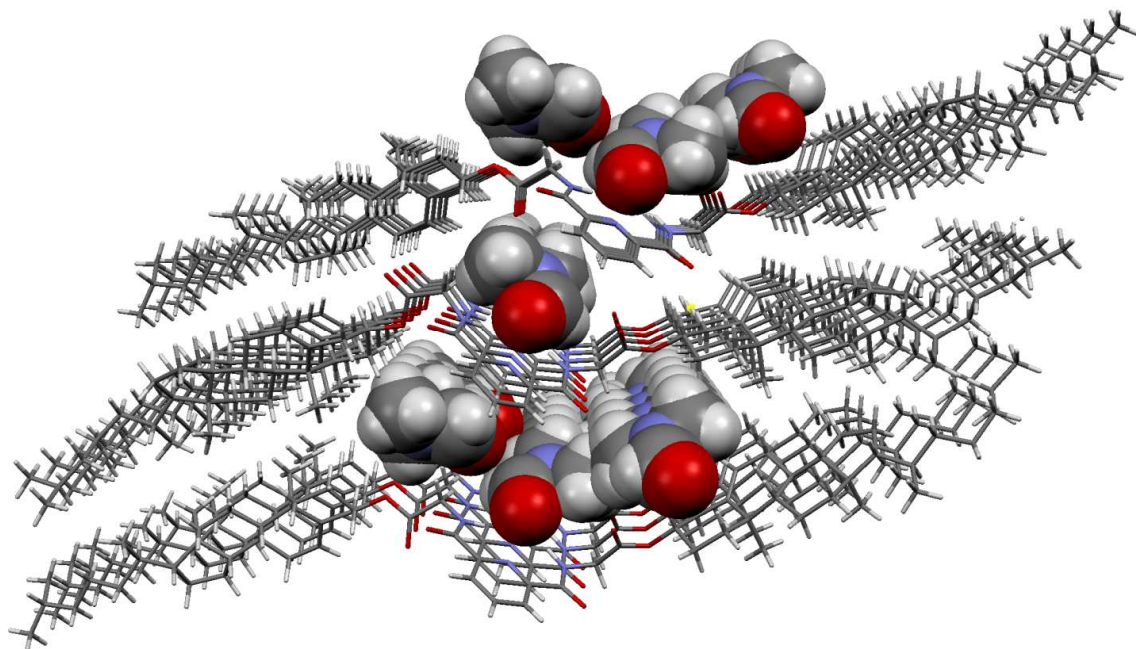


Fig. S26 Two distinct solvent filled voids between sheets of gelator molecules.

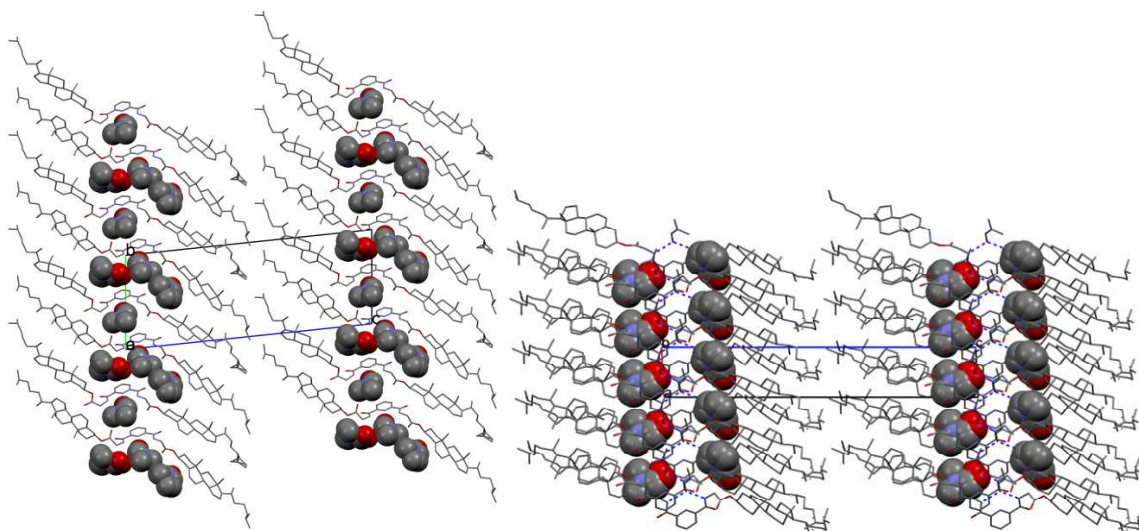


Fig. S27 Stacking order of the DMF filled voids shown along *a*- axis (left) and *b*-axis (right).

Table S2 Crystal data and refinement parameters.

Identification code	1 DMF
Empirical formula	C ₁₄₂ H ₂₂₆ N ₁₀ O ₁₆
Formula weight	2329.33
Temperature/K	123.00(10)
Crystal system	triclinic
Space group	P1
a/Å	6.1385(2)
b/Å	14.6387(5)
c/Å	37.9634(9)
α/°	83.436(2)
β/°	86.000(3)
γ/°	80.353(3)
Volume/Å ³	3336.62(17)
Z	1
ρ _{calc} /mg/mm ³	1.159
m/mm ⁻¹	0.585
F(000)	1276.0
Crystal size/mm ³	0.332 × 0.1202 × 0.0264
2θ range for data collection	6.16 to 139°
Index ranges	-7 ≤ h ≤ 7, -17 ≤ k ≤ 16, -46 ≤ l ≤ 46
Reflections collected	56055
Independent reflections	23877[R(int) = 0.0551]
Data/restraints/parameters	23877/122/1592
Goodness-of-fit on F ²	1.017
Final R indexes [I >= 2σ (I)]	R ₁ = 0.0716, wR ₂ = 0.1819
Final R indexes [all data]	R ₁ = 0.0979, wR ₂ = 0.2056
Largest diff. peak/hole / e Å ⁻³	1.38/-0.40
Flack parameter	-0.3(2)
CCDC number*	883809

* = CCDC 883809 contains the supplementary crystallographic data for this paper. These data can be obtained free of charge from The Cambridge Crystallographic Data Centre via www.ccdc.cam.ac.uk/data_request/cif.

Table S3 Selected bond distances and angles.

	D...A (Å)	D-H...A (°)	(°)
<i>D-H...A</i>			
N9-H9...O153	3.088(6)	156	
N43-H43...O153	2.945(6)	159	
N83-H83...O158	2.932(5)	151	
N117-H117...O158	3.009(5)	160	
dihedral angles			
C7-N9-C10-C11			-60.9(8)
C41-N43-C44-C45			-77.0(6)
C81-N83-C84-C85			-61.1(5)
C115-N117-C118-C119			-69.7(5)